38. Dong X, Storkus WJ, Salter RD. Binding and uptake of agalactosyl IgG by mannose receptor on macrophages and dendritic cells. J Immunol 1999;163:5427–34.
39. Rudd PM, Elliott T, Cresswell P, et al. Glycosylation and the immune system. Science 2001;291:2370–6.

CONFLICT OF INTEREST

Guarantor of the article: Hideki Iijima, M.D., Ph.D.
Specific author contributions: Conception and design: Hideki Iijima, Eiji Miyoshi, and Norio Hayashi; biochemical analysis: Shinichiro Shinzaki, Takatoshi Nakagawa, Sachiko Nakajima, Akihiro Kondo, and Eiji Miyoshi; sample collection and clinical data analysis: Satoshi Egawa, Shuji Ishii, Takanobu Irie, Yoshimi Kakiuchi, Tsutomu Nishida, Masakazu Yasumaru, Tsunekazu Mizushima, Harumasa Yoshihara, Tatsuya Kanto, Masahiko Tsujii, and Shingo Tsuji; and manuscript preparation: Shinichiro Shinzaki, Hideki Iijima, Takatoshi Nakagawa, Masahiko Tsujii, Akihiro Kondo, and Eiji Miyoshi.
Financial support: This work was supported by a Grant-in-Aid from the Japan Society for the Promotion of Science (18590680 and 19590721) and a Grant-in-Aid for Smoking Research Foundation.
Potential competing interests: None.

THE JOURNAL OF BIOLOGICAL CHEMISTRY VOL. 283, NO. 39, pp. 26820–26828, September 26, 2008

Fusion of OTT to BSAC Results in Aberrant Up-regulation of Transcriptional Activity*[S]

Received for publication, March 25, 2008, and in revised form, July 21, 2008 Published, JBC Papers in Press, July 30, 2008 DOI 10.1074/jbc.M802315200

Taisuke Sawada[‡], Chiharu Nishiyama[§], Takuma Kishi[‡], Tomonari Sasazuki[‡], Sachiko Komazawa-Sakon[‡], Xin Xue[‡], Jiang-Hu Piao[‡¶‖], Hideko Ogata[‡], Jun-ichi Nakayama[**], Tomohiko Taki[‡‡], Yasuhide Hayashi[§§], Mamoru Watanabe[¶¶], Hideo Yagita[‡], Ko Okumura[‡], and Hiroyasu Nakano[‡1]

From the [‡]Department of Immunology, [§]Atopy (Allergy) Research Center, and [¶]Sportology Center, Juntendo University School of Medicine, 2-1-1 Hongo, Bunkyo-ku, Tokyo 113-8421, Japan, the [‖]Department of Immunology, School of Basic Medical Science, Ningxia Medical College, Xingqing-Qu, Yinchuan 750004, China, the [**]Laboratory for Chromatin Dynamics, Center for Developmental Biology, RIKEN, 2-2-3 Minatojima-Minamimachi, Chuo-ku, Kobe 650-0047, Japan, the [‡‡]Department of Molecular Laboratory Medicine, Kyoto Prefectural University of Medicine Graduate School of Medical Science, 465 Kajii-cho kawaramachi-Hirokoji, Kamigyo-ku, Kyoto 602-8566, Japan, the [§§]Gunma Children's Medical Center, 779 Shimohakoda, Kitatachibana, Gunma 377-8577, Japan, and the [¶¶]Department of Gastroenterology and Hepatology, Tokyo Medical and Dental University, 1-5-45 Yushima, Bunkyo-ku, Tokyo 113-8519, Japan

***OTT/RBM15-BSAC/MAL/MKL1/MRTF-A* was identified as a fusion transcript generated by t(1;22)(p13;q13) in acute megakaryoblastic leukemia. Previous studies have shown that BSAC (basic, SAP, and coiled-coil domain) activates the promoters containing CArG boxes via interaction with serum response factor, and OTT (one twenty-two) negatively regulates the development of megakaryocytes and myeloid cells. However, the mechanism by which OTT-BSAC promotes leukemia is largely unknown. Here we show that OTT-BSAC, but not BSAC or OTT strongly activates several promoters containing a transcription factor Yin Yang 1-binding sequence. In addition, although BSAC predominantly localizes in the cytoplasm and its nuclear translocation is considered to be regulated by the Rho-actin signaling pathway, OTT-BSAC exclusively localizes in the nucleus. Moreover, OTT interacts with histone deacetylase 3, but this interaction is abolished in OTT-BSAC. Collectively, these functional and spatial changes of OTT and BSAC caused by the fusion might perturb their functions, culminating in the development of acute megakaryoblastic leukemia.**

Transcriptional activation of many genes depends on activities of the transcriptional factors that recognize specific target sequences but also the chromatin structures. Histone acetyltransferases and histone deacetylases (HDACs)[2] are recruited to target genes through association with specific transcriptional factors (1, 2). Histone acetyltransferases relax chromatin structures and activate transcription by acetylating histones, whereas HDACs condense chromatin structures and repress transcription by deacetylating histones (1, 2). So far, there have been three HDAC families identified (3). Class I HDACs (HDAC1, -2, -3, and -8) are closely related to the yeast transcriptional regulator RPD3 and expressed in most cell types. Class II HDACs (HDAC4, -5, -6, -7, -9, and -10) share domains with a similarity to HDA1, another deacetylase in yeast. Class III HDACs are related to the yeast silencing protein SIR2 and are dependent on NAD for enzymatic activity. HDACs exist in cells as a part of large molecular weight complex containing adaptor molecules, including Sin3A, SMRT (silencing mediator for retinoid and thyroid receptors), N-CoR (nuclear receptor corepressor), and/or SHARP (SMRT and HDAC1-associated repressor protein) (4). SHARP belongs to a family of RNA recognition motif proteins and also has a SMRT-interacting domain at the C terminus, which mediates the interaction with SMRT, N-CoR, and HDACs (5). The SMRT-interacting domain is also characterized as a SPOC (spen paralog and ortholog C-terminal) domain that was found in *Drosophila* spen and spen-like protein (6).

The t(1;22)(p13;q13) is exclusively associated with infant acute megakaryoblastic leukemia. Two groups have been independently identified as a fusion transcript that is generated by this chromosomal translocation and composed of two novel genes, designated OTT (one twenty-two) or RNA-binding motif protein (RBM) 15 and megakaryocytic acute leukemia (MAL) or megakaryoblastic leukemia-1(MKL1) (7, 8). OTT contains three RNA recognition motifs and SPOC domain (7, 8), whereas MAL is composed of N-terminal basic, glutamine-

* This work was supported in part by a Grant-in-Aid for a "High-Tech Research Center" Project for Private Universities, matching fund subsidy from the Ministry of Education, Culture, Sports, Science and Technology, and Scientific Research (B) and (C) from Japan Society for the Promotion of Science, and grants from the NOVARTIS Foundation (Japan) for the Promotion of Science, the Takeda Science Foundation, the Mitsubishi Pharma Foundation, and the Tokyo Biochemical Research Foundation. The costs of publication of this article were defrayed in part by the payment of page charges. This article must therefore be hereby marked "*advertisement*" in accordance with 18 U.S.C. Section 1734 solely to indicate this fact.

[S] The on-line version of this article (available at http://www.jbc.org) contains supplemental Fig. S1.

[1] To whom correspondence should be addressed: Dept. of Immunology, Juntendo University School of Medicine, 2-1-1 Hongo, Bunkyo-ku, Tokyo 113-8421, Japan. Tel.: 81-3-5802-1045; Fax: 81-3-3813-0421; E-mail: hnakano@juntendo.ac.jp.

[2] The abbreviations used are: HDAC, histone deacetylase; ChIP, chromatin immunoprecipitation; YY1, Yin Yang 1; MAL, megakaryocytic acute leukemia; MKL1, megakaryoblastic leukemia-1; RBM, RNA-binding motif protein; GPVI, platelet collagen receptor glycoprotein VI; EMSA, electrophoretic mobility shift assay; SRF, serum response factor; siRNA, small interfering RNA; TA, transcriptional activation.

rich, SAP (SAF-A/B, Acinus, PIAS), and coiled-coil domains (7, 8). OTT-MAL encodes a fusion protein containing complete domain structures of both OTT and MAL. However, the molecular mechanism whereby this fusion protein induces leukemia is largely unknown. On the other hand, we and others have independently identified a murine homolog of MAL, referred to as BSAC and MRTF-A by functional cloning to inhibit tumor necrosis factor α-induced cell death and bioinformatics to identify related genes to myocardin, respectively (9, 10). Accumulating studies have shown that BSAC/MAL/MKL1/MRTF-A activates the promoters containing CArG boxes ($CC(A/T)_6GG$) through associating with serum response factor (SRF) (9–11). In addition, nuclear translocation of BSAC is tightly regulated by the Rho-actin signaling pathway (12). Although *BSAC/MAL/MKL1/MRTF-A* and *SRF* are broadly expressed in various tissues, the defect of *MKL1/MRTF-A*$^{-/-}$ mice is unexpectedly restricted to the development of the mammary gland (13, 14).

Yin Yang 1 (YY1) is a ubiquitous zinc finger transcription factor that binds to many different cellular and viral promoters in a sequence-specific manner to regulate transcription (15, 16). The mechanism by which YY1 activates or represses transcription largely depends on the interaction with other transcription factors or histone modification enzymes including TBP, TAFs, SP1, p300, and HDACs (15, 16). Importantly, the targeted disruption of *YY1* resulted in preimplantation lethality, indicating that YY1 is essential for mouse embryo development (17). Moreover, subcellular localization of YY1 is regulated in a cell cycle-dependent fashion and modulates the function of the cell cycle control genes including *Rb* and *p53*. Furthermore, a recent study has revealed that perturbed expression of YY1 inhibits maturation of granulocytes, suggesting an intimate link with the development of acute myeloid leukemia (18). Collectively, YY1 potentially controls the expression of vast array of genes that are important in basic cellular processes such as DNA replication, transcription, and cell cycle control and also involved in the leukemogenesis.

Given that the promoters containing CArG boxes are found in immediate early genes or muscle-specific genes and OTT-BSAC is involved in the development of leukemia, we speculated that OTT-BSAC activates promoter(s) containing a motif other than CArG box. We found that OTT-BSAC strongly activated the promoters of human platelet collagen receptor glycoprotein VI (*GPVI*) gene. Deletion and mutation analysis revealed that OTT-BSAC-mediated transcriptional activity depended on the YY1-binding sequences. Interestingly, in contrast to BSAC, which predominantly localized in the cytoplasm and the nuclear translocation of which is tightly regulated by the Rho-dependent signals (12), OTT and OTT-BSAC exclusively localized in the nucleus. The constitutive nuclear accumulation of OTT-BSAC may contribute to a significant enhancement of its transcriptional activity. Moreover, OTT interacted with HDAC3, and this interaction was abolished in OTT-BSAC. Collectively, these functional and spatial alterations of OTT and BSAC may culminate in the development of leukemia.

EXPERIMENTAL PROCEDURES

Reagents and Cell Culture—Anti-FLAG (Sigma-Aldrich), anti-hemagglutinin (Roche Applied Science), anti-Myc, anti-GAL4, and anti-YY1 (Santa Cruz Biotechnology), anti-HDAC3 (Biomol), anti-β-actin (BioLegend) antibodies, control mouse IgG (BD Biosciences), and control rabbit IgG (Sigma-Aldrich) were purchased from the indicated sources. HEK293 and HEK293T cells were cultured in high glucose Dulbecco's modified Eagle's medium containing 10% fetal calf serum. Megakaryocytic leukemic cell lines, CMS and CMY (T. Sato), and MEG-01 cells (M. Seto) (19) were kindly provided and cultured in RPMI1640 medium containing 10% fetal calf serum. Anti-OTT antibody was generated by immunizing rabbits with GST-OTT (609–730). Anti-BSAC antibody was generated and described previously (9).

Plasmids—pBJ5-FLAG-HDAC1 (S. Schreiber), pME18S-FLAG-HDAC2 and pCEP4-FLAG-HDAC3 (E. Seto), and pCMX-mSMRTα-FL (R. M. Evans) were kindly provided from the indicated researchers. pCR-FLAG-YY1 was constructed by PCR using pCR-YY1 as a template (20). pCR-FLAG-HDAC3ΔN and pCR-FLAG-HDAC3ΔC were constructed by deleting N-terminal 307 and C-terminal 121 amino acids using PCR, respectively. A full-length *OTT* cDNA was isolated by screening a library derived from human HTLV-1-transformed T cell line HAT109 as a standard procedure. To express full-length and various deletion mutants of OTT as fusion proteins with DNA-binding domain of a yeast transcriptional factor GAL4, PCR products encoding the indicated amino acids were subcloned into pFA vector (Stratagene), designated as pFA-OTT, pFA-OTT(1–677), pFA-OTT(654–957), pFA-OTT(609–730), and pFA-OTT(1–533). pcDNA3-Myc-OTT was constructed by PCR and subcloned into pcDNA3-Myc vector. pcDNA3-Myc-human BSAC and pCR-FLAG-human HDAC6 were constructed by PCR using KIAA1438 (human *BSAC/MAL/MKL1/MRTF-A*) and KIAA0901 (human *HDAC6*) cDNAs derived from the Kazusa DNA Institute as templates, respectively. To make an expression vector for OTT-BSAC, PCR products of *OTT* and *BSAC* were connected by creating an additional EcoRI site at the fusion junction and ligated to pcDNA3-Myc vector. The artificially created EcoRI site was subsequently mutated to the originally published sequence of the *OTT-BSAC* fusion junction using a QuikChange site-directed mutagenesis kit (Stratagene). Expression vectors for C-terminal deletion mutants of OTT-BSAC (−351) and OTT-BSAC (−537) were constructed by using the internal restriction enzyme sites XmnI and BsgI to delete C-terminal fragments, respectively. The numbers indicate deleted amino acids from the C terminus of OTT-BSAC.

Reporter Assay—The promoter of the human *GPVI* gene (−315 to +29) was amplified by PCR using human genomic DNA as a template and subcloned into pGL3-basic vector (Promega), designated as pGL3-*GPVI* (−315/+29). A series of 5′ deletion mutants, pGL3-*GPVI* (−207/+29), pGL3-*GPVI* (−79/+29), and pGL3-*GPVI* (−39/+29) were generated by PCR using pGL3-*GPVI* (−315/+29) as a template. pGL3-*GPVI* (−208/+29M1), pGL3-*GPVI* (−208/+29M2), and pGL3-*GPVI* (−79/+29M3) were generated by introducing mutations

of GATA (AGATAA to CGCTTA), the first YY1 (GATGAG to GCTTAG), and third YY1 (CTCATC to CTAAGC) binding sites, respectively. Reporter plasmids, pGL3-c-*fos* (−700/+53), pGL3-*FcεRIα* (−605/+29), and mPGV-B-*il-6* (−181/+14) were described previously (9, 20, 21). Luciferase assays using HEK293 and HEK293T cells were performed as previously described (22). MEG-01 cells (2×10^5) were transfected with the indicated expression vectors along with reporter plasmids using Lipofectamine 2000 (Invitrogen). After 48 h, the cells were harvested, and the luciferase activities were measured on a luminometer (Berthold).

Electrophoretic Mobility Shift Assay (EMSA)—EMSA was performed as previously described (20). Briefly, 5 μg of the nuclear extracts were incubated with the rhodamine-labeled wild-type oligonucleotides in the absence or presence of anti-YY1 antibody, wild-type, or mutant cold competitors with a 10–100-fold excess. The oligonucleotides used were as follows: wild-type sense oligonucleotide for *GPVI*, 5′-AGGAAGGGAGGAGAGCATTCTTC-ATCCTCATCACATCCTG-3′; mutant sense oligonucleotide, 5′-AGGAAGGGAGGAGAGCATTCTTCATCCTAAGCGCA-TCCTG-3′. Mobility shift of the complexes was analyzed by a fluorescence detector, FMBIO-100 (Takara Shuzo).

Chromatin Immunoprecipitation (ChIP) Assay—The ChIP assay was performed using a ChIP Assay kit (Millipore) as previously described (23). Quantitative PCRs were performed using TaqMan Universal PCR master mix and a 7500 Real-Time PCR system (Applied Biosystems). The primers to amplify the promoter region of *GPVI* gene (−127/+29) and a TaqMan probe were as follows: Forward primer (5′-GGCTA-CGGCTCGATGAGTCTC-3′), reverse primer (5′-TCAGCC-CTGTCCTGAGCTCT-3′), and a TaqMan probe (5′-FAM-TTCATCCTCATCACATCC-MGB-3′). The amount of target DNA bound to YY1 or OTT-BSAC was quantified using immunoprecipitates with control, anti-YY1, or anti-Myc antibodies from the cycle threshold value, which was determined using 7500 SDS software (Applied Biosystems). In brief, the ratio of the amount of a specific DNA fragment in each immunoprecipitate to the amount of that fragment in the DNA before immunoprecipitation (input DNA) was calculated from each cycle threshold value.

Subcellular Fractionation, Immunoprecipitation, and Immunoblotting—HEK293 cells (4×10^6) were transiently transfected with the indicated expression vectors using Lipofectamine (Invitrogen). MEG-01 cells (4×10^6) were untreated or transfected with the indicated expression vectors using a nucleofector according to the manufacturer's instructions (Amaxa). For subcellular fractionation, the cells were harvested at 24–36 h after transfection and washed with 1 ml of a buffer A (10 mM Hepes, pH 7.9, 1.5 mM $MgCl_2$, 10 mM KCl, 1 μg/ml aprotinin, 1 μg/ml leupeptin, 1 mM dithiothreitol, and 1 mM phenylmethylsulfonyl fluoride) and then resuspended in 500 μl of the buffer A. After incubation for 30 min, the cells were passed with a 30-gauge syringe 10 times, followed by centrifugation at 700 × *g*. The supernatants were further centrifuged at 15,000 × *g* to remove insoluble pellets, and the resulting supernatants were collected as the cytoplasmic fractions. The pellets were resuspended in 100 μl of buffer B (20 mM Hepes, pH 7.9, 450 mM NaCl, 1.5 mM $MgCl_2$, 25% glycerol, 0.2 mM EDTA, 1 μg/ml aprotinin, 1 μg/ml leupeptin, 1 mM dithiothreitol, and 1 mM phenylmethylsulfonyl fluoride) for 60 min. After centrifugation at 15,000 × *g* for 10 min, the supernatants were collected as the nuclear fractions. Equal amounts of proteins from each fraction were subjected to SDS-PAGE and transferred onto polyvinylidine difluoride membranes (Millipore). The membranes were incubated with the indicated antibodies followed by the corresponding secondary antibodies. The membranes were then developed with the ECL Western Blotting Detection System Plus (GE Healthcare).

Small Interfering RNAs (siRNAs)—HEK293T cells (2.5×10^5) were transfected with siRNAs targeting green fluorescent protein (control) or *YY1* (ON-TARGETplus SMARTpool siRNA, Dharmacon) and pGL3-*GPVI* (−315/+29) along with Myc-OTT-BSAC using Lipofectamine 2000 (Invitrogen). After 48 h, knockdown of YY1 was evaluated by immunoblotting with anti-YY1 antibody using total lysates, and luciferase assay was performed as previously described (22).

Immunostaining—MEG-01 cells (4×10^6) were untreated or transfected with the indicated expression vectors and plated on glass slides. After 24 h, the cells were washed with phosphate-buffered saline, fixed with 2% paraformaldehyde, and then incubated with anti-OTT, anti-BSAC, and anti-Myc antibodies. The primary antibodies were detected by secondary antibodies conjugated with Alexa 488 or Alexa 594 (Invitrogen). To visualize the nuclei, the cells were incubated with Hoechst 33258 (Invitrogen). Stained cells were mounted in SlowFade (Invitrogen) and analyzed on a laser scanning confocal microscope (Zeiss).

RESULTS

Identification of a Novel Target Gene Activated by the Fusion Protein OTT-BSAC—OTT-MAL encodes a fusion protein containing complete domain structures of both OTT and MAL (Fig. 1*A*). However, the molecular mechanism whereby this fusion protein induces leukemia is largely unknown. Given that CArG boxes are found in the promoters of immediate early genes or muscle-specific genes, we speculated that OTT-BSAC should control gene(s) that might be responsible for the development of leukemia. Given that OTT-BSAC might impair the differentiation of megakaryocytes, we first tested whether OTT-BSAC could affect the promoter activity of megakaryocyte-specific genes. A previous study has shown that *GPVI* is specifically expressed in megakaryocytes and platelets (24). Then we generated a reporter plasmid containing the *GPVI* promoter upstream of a luciferase gene. We transfected megakaryocytic leukemic cell line MEG-01 cells with expression vectors for BSAC, OTT, and OTT-BSAC along with a reporter plasmid, pGL3-*GPVI* (−315/+29), and tested the effect of each protein on this promoter activity. Expression of BSAC or OTT did not significantly increase this promoter activity (Fig. 1*B*), which is consistent with the fact that this promoter does not contain a CArG box. Surprisingly, expression of OTT-BSAC strongly activated this promoter in a dose-dependent fashion (Fig. 1*B*). This OTT-BSAC-mediated transcriptional activation of the *GPVI* promoter was also observed in HEK293 cells (Fig. 1*B*). To investigate whether OTT-BSAC-dependent transcriptional activity on the *GPVI* promoter is

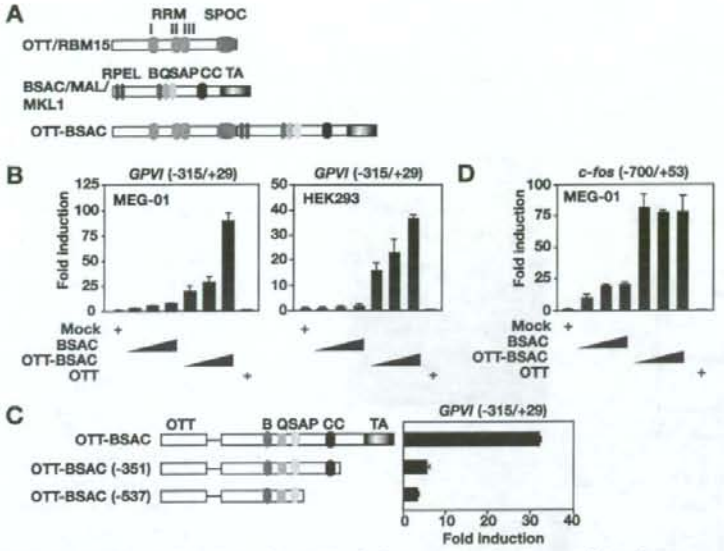

FIGURE 1. **OTT-BSAC strongly activates the *GPVI* and c-*fos* promoters.** *A*, a diagram of domain structures of OTT/RBM15, BSAC/MAL/MKL1/MRTF-A, and OTT-BSAC. RNA recognition motif, SPOC, RPEL, basic (*B*), glutamine-rich (*Q*), SAP, coiled-coil (*CC*), and TA domains are shown. *B*, MEG-01 and HEK293 cells were transfected with increasing amounts of the indicated expression vectors along with pGL3-*GPVI* (−315/+29). Luciferase activities are expressed as fold increases above that with control vector. Each experiment was performed in triplicate, and the results are expressed as the means ± SE of three experiments. *C*, MEG-01 cells were transfected activities are expressed as in *B*. *D*, MEG-01 cells were transfected with increasing amounts of the indicated expression vectors along with pGL3-c-*fos* (−700/+53). Luciferase activities are expressed as in *B*.

mediated by the transcriptional activation (TA) domain of BSAC, we transfected MEG-01 cells with deletion mutants of OTT-BSAC lacking the TA domain. Although the expression levels of two OTT-BSAC mutants lacking the TA domain were comparable with OTT-BSAC (supplemental Fig. S1), two mutants failed to activate this promoter (Fig. 1*C*). This indicates that the TA domain of BSAC mediates transcriptional activity of OTT-BSAC. Given that protein expression levels of OTT-BSAC were consistently lower than BSAC, possibly because of its large molecular mass of OTT-BSAC (supplemental Fig. S1), increased transcriptional activity of OTT-BSAC is not due to the increased protein expression levels. Consistent with a previous study (11), we also observed significant enhancement of transcriptional activity of OTT-BSAC on the c-*fos* promoter compared with BSAC (Fig. 1*D*). Given that the *GPVI* but not c-*fos* promoter does not contain CArG box, these results suggest that OTT may directly or indirectly recruit BSAC to the *GPVI* promoter, resulting in up-regulation of the *GPVI* promoter activity.

Transcriptional Activation by OTT-BSAC Depends on the YY1-binding Sequences—To identify a target sequence recognized by OTT-BSAC, we constructed a series of 5′ deletion mutants of the *GPVI* promoter (Fig. 2*A*). Although deletion up to the position −208 did not impair the transcriptional activity induced by OTT-BSAC, further deletion up to −80 reduced the transcriptional activity to ~50% (Fig. 2*B*). Moreover, deletion up to −40 resulted in complete loss of the transcriptional activation. These results indicate that the regions spanning −207 to −80 and −79 to −40 are essential for OTT-BSAC-mediated transactivation. A previous study has shown that the *GPVI* promoter activity is regulated by Sp1, GATA, and Ets motifs (24). In addition, we found three putative YY1-binding sequences (designated as YY1-I, YY1-II, and YY1-III) in the *GPVI* promoter (Fig. 2*A*). We tested whether the mutation of these sites impairs OTT-BSAC-mediated transactivation. The mutation of the GATA-binding sequence did not reduce but rather enhanced the transcriptional activity. Unexpectedly, mutation of YY1-I reduced the transcriptional activity comparable with a deletion mutant (−79/+29) (Fig. 2*B*). Furthermore, the mutation of YY1-III substantially reduced the transcriptional activity 5-fold. Notably, combined mutations of YY1-III along with Ets motifs or YY1-II did not further reduce the transcriptional activity compared with YY1-III mutation alone (data not shown). Combining these data together indicates that YY1-I and YY1-III sequences are essential for OTT-BSAC-dependent transcriptional activation.

We next tested whether YY1 actually binds to the promoter by EMSA. We prepared the nuclear extracts from MEG-01 cells and performed EMSA using double-stranded oligonucleotides (oligonucleotides) containing a region spanning −79 to −40 as a probe. As shown in Fig. 2*C*, two major retarded bands (designated the complex I and II hereafter) were detected in this assay, and these two bands disappeared by the addition of the nonlabeled wild-type oligonucleotides. In contrast, the addition of the mutant probe, in which YY1-binding core sequence (TCAT) was mutated to TAAG, did not abolish the binding of the two complexes to the labeled oligonucleotides, indicating that these complexes specifically bound to TCAT sequence. Moreover, complex II but not complex I disappeared in the presence of anti-YY1 antibody, suggesting that complex II contains YY1. Collectively, YY1 binds to the *GPVI* promoter via TCAT sequence. However, we could not detect direct interaction of YY1 with BSAC or OTT in cotransfection experiments or a ternary complex containing YY1 and BSAC or OTT-BSAC in the presence of YY1-binding sequence in EMSAs (data not shown).

To directly show that endogenous YY1 is recruited to the *GPVI* promoter under more physiological conditions, we performed ChIP assays. Consistent with EMSAs, anti-YY1 but not control antibody efficiently immunoprecipitated the *GPVI* promoter from HEK293T and MEG-01 cells (Fig. 2*D*). However, the relative intensities of the *GPVI* promoter using immunoprecipitates with anti-Myc antibody were not different in between mock and Myc-OTT-BSAC-transfected HEK293T cells (Fig. 2*E*). This suggests that the recruitment of transfected

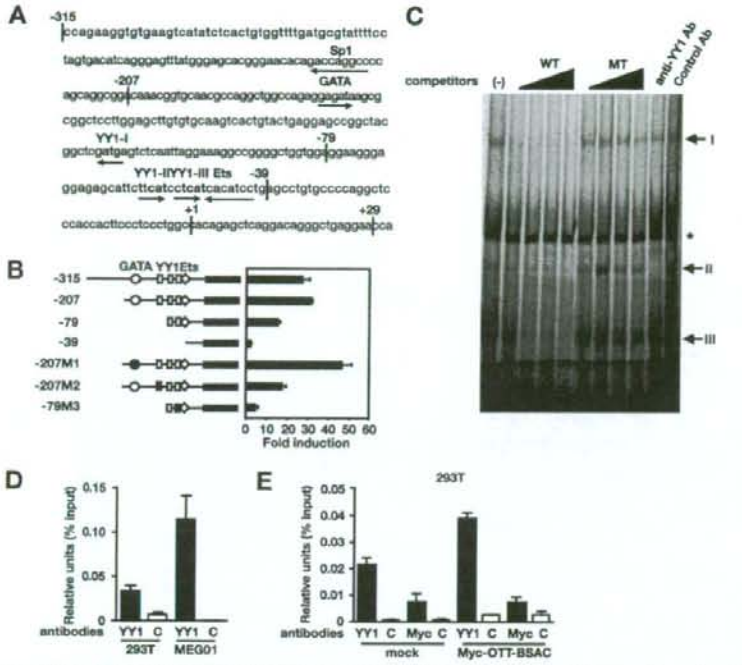

FIGURE 2. **OTT-BSAC activates the *GPVI* promoter via the YY1-binding motifs.** *A*, the promoter region of human *GPVI* gene. The putative transcriptional factor binding sites are *underlined* by the *arrows* showing its orientation (sense or antisense orientation). *+1* indicates the transcription start site. The putative YY1-binding sequences are indicated by *bold characters*. *B*, delineation of the regions required for OTT-BSAC-dependent transactivation. MEG-01 cells were transfected with OTT-BSAC along with the indicated mutants of pGL3-*GPVI* reporter vector. Luciferase activities are expressed as in Fig. 1*B*. *M1*, *M2*, and *M3* are the mutants, in which GATA1, the first YY1, and third YY1 motifs were mutated, respectively. *C*, YY1 specifically binds to the promoter of *GPVI*. The nuclear extracts were incubated with the rhodamine-labeled wild-type oligonucleotides containing the *GPVI* promoter (−79 to −39) in the absence or presence of increasing amounts of the nonlabeled wild-type (*WT*) or mutant (*MT*) oligonucleotides or anti-YY1 or control antibodies. The retarded bands are indicated by *arrows*. The *asterisk* indicates nonspecific bands. *D*, *in vivo* binding of YY1 to the *GPVI* promoter in HEK293T and MEG-01 cells. The binding of YY1 to the *GPVI* promoter region (−127/+22) was quantified using ChIP assays. The results are expressed as the means ± S.D. of three independent PCRs with duplicates samples. *E*, OTT-BSAC does not bind to the *GPVI* promoter *in vivo*. Mock or Myc-OTT-BSAC-transfected HEK293T cells were subjected to ChIP assays using anti-YY1, anti-Myc, or control antibodies. The results are expressed as in *D*.

OTT-BSAC to the *GPVI* promoter could not be detected, at least under our experimental conditions.

YY Is Not Essential for OTT-BSAC-dependent Transcriptional Activation—Previous studies have shown that myocardin and BSAC do not directly bind to the promoters containing CArG boxes but activates them through interaction with SRF (9–11). Under these conditions, transcriptional activities by myocardin and BSAC are extremely sensitive to the levels of SRF, because high concentration of SRF does not enhance but rather attenuates myocardin- or BSAC-dependent transcriptional activation (25).[3] To test whether similar interplay between OTT-BSAC and YY1 is also observed on the *GPVI* promoter, we examined whether expression of YY1 attenuates OTT-BSAC-dependent transactivation. Although expression of YY1 alone weakly activated this promoter, expression of YY1 substantially inhibited OTT-BSAC-mediated transcriptional activation in a dose-dependent fashion (Fig. 3*A*). Notably, this inhibitory effect of YY1 was promoter-specific, because expression of YY1 only weakly inhibited OTT-BSAC-dependent transactivation on the c-*fos* promoter (Fig. 3*B*). We confirmed that the expression levels of transfected YY1 in the *GPVI* promoter-transfected MEG-01 cells were nearly identical to those of c-*fos* promoter-transfected MEG-01 cells (Fig. 3*C*).

The fact that YY1 substantially suppressed OTT-BSAC-mediated transcriptional activation raises two possibilities. One is that YY1 may recruit OTT-BSAC to the *GPVI* promoter, although the recruitment of transfected OTT-BSAC to the *GPVI* promoter was not detected under our experimental conditions (Fig. 2*E*). The other is that a transcription factor other than YY1 recruits OTT-BSAC to the YY1-binding sequences and activates the *GPVI* promoter; therefore YY1 appears to suppress OTT-BSAC-dependent transcriptional activation through competitive binding inhibition (Fig. 3*A*). To discriminate these two possibilities, we knocked down endogenous YY1 using siRNA and tested whether OTT-BSAC-dependent transcriptional activation is abolished in YY1-knockdown HEK293T cells. Although *YY1* siRNA efficiently knocked down expression of YY1, OTT-BSAC-mediated transcriptional activation was not impaired (Fig. 3*D*). Collectively, OTT-BSAC activates transcription on the *GPVI* promoter through the YY1-binding sequences, but YY1 is not essential for OTT-BSAC- mediated transcriptional activation.

We finally investigated whether OTT-BSAC activates other promoters containing the YY1-binding sequences. We have previously shown that the human *FcεRIα* subunit promoter contains the YY1-binding sequences and is activated by YY1 (20). Thus, we tested whether expression of OTT-BSAC activates this promoter. As expected, OTT-BSAC substantially increased this promoter activity (Fig. 3*E*). We also found that OTT-BSAC activates the murine *il-6* promoter, which also contains the YY1-binding sequences (Fig. 3*E*).

The Signal-independent Nuclear Accumulation of OTT-BSAC—To elucidate the mechanism whereby transcriptional activity of OTT-BSAC is enhanced compared with BSAC, we speculated that OTT fusion to BSAC could affect the subcellular localization of BSAC. We first examined the subcellular

[3] T. Sawada and H. Nakano, unpublished results.

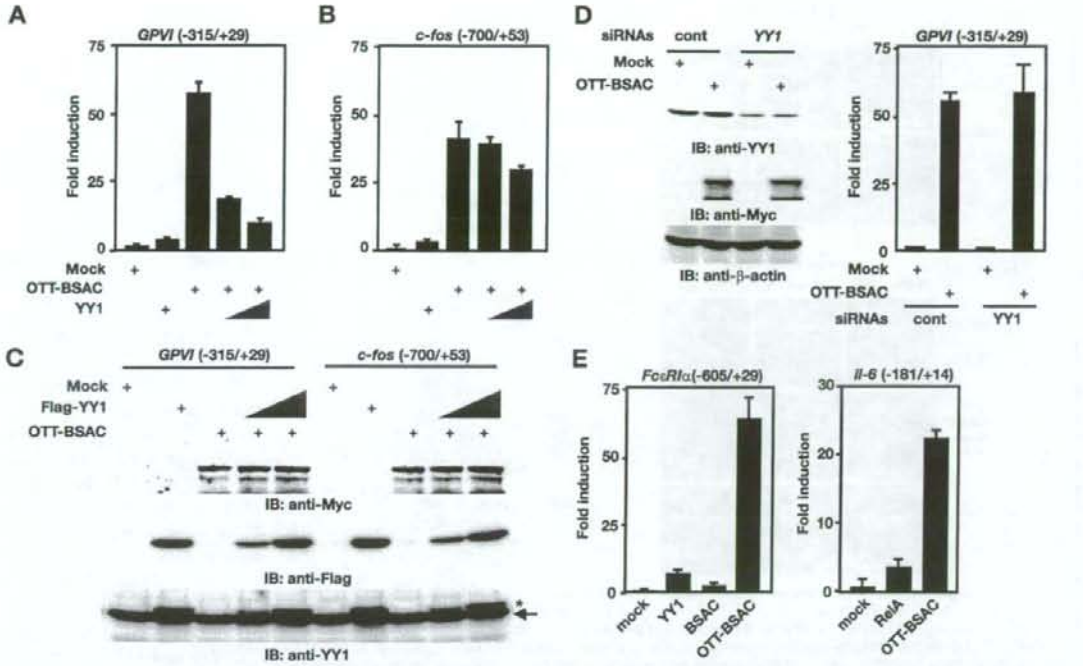

FIGURE 3. **YY is not essential for OTT-BSAC-mediated transcriptional activation.** *A–C*, MEG-01 cells were transfected with Myc-OTT-BSAC and pGL3-*GPVI* (−315/+29) (*A* and *C*) or pGL3-*c-fos* (−700/+53) (*B* and *C*) along with increasing amounts of FLAG-YY1. The luciferase activities are expressed as in Fig. 1*B*. *C*, expression levels of transfected proteins and endogenous YY1 were detected by immunoblotting (*IB*) with anti-Myc, anti-FLAG, and anti-YY1 antibodies. The *arrow* and *asterisk* indicate endogenous and transfected YY1, respectively. *D*, knockdown of YY1 using siRNA does not impair OTT-BSAC-dependent transcriptional activation. HEK293T cells were transfected with siRNAs targeting green fluorescent protein (control) or *YY1* and pGL3-*GPVI* (−315/+29) along with an empty vector (mock) or Myc-OTT-BSAC. After 48 h, the expression levels of endogenous YY1 and transfected OTT-BSAC were detected by immunoblotting with anti-YY1 (*top panel*) and anti-Myc antibodies (*middle panel*), respectively. The equal loading of the samples was verified by immunoblotting with anti-β-actin antibody (*bottom panel*). The luciferase activities are expressed as in Fig. 1*B*. *E*, MEG-01 cells were transfected with the indicated expression vectors along with pGL3-*FcεRIα* (−605/+29) or mPGV-B-*il-6* (−181/+14). The luciferase activities are expressed as in Fig. 1*B*.

localization of endogenous BSAC and OTT in MEG-01 cells. Consistent with a previous study (12), endogenous BSAC predominantly localized in the cytoplasm with a minor population in the nucleus (Fig. 4*A*). To investigate the subcellular localization of endogenous OTT, we generated anti-OTT antibody. This antibody recognized endogenous OTT with a molecular mass of 120 kDa in the whole cell lysates from MEG-01, HeLa, HEK293, and Jurkat T, but not CMS or CMY cells (Fig. 4*C*). Consistent with a very recent study, in which ectopically expressed OTT localizes in the nucleus (26), endogenous OTT localized in the nucleus (Fig. 4*A*). Similarly, transfected BSAC and OTT showed identical subcellular distribution patterns to endogenous BSAC and OTT, respectively (Fig. 4*B*). We finally investigated the localization of OTT-BSAC. Because leukemia cell line(s) from patients with acute megakaryoblastic leukemia are not currently available, we transiently transfected MEG-01 cells with Myc-OTT-BSAC. Interestingly, OTT-BSAC exclusively localized in the nucleus (Fig. 4*B*).

To evaluate the subcellular localization of OTT, BSAC, and OTT-BSAC more quantitatively, we separated the cells into the cytoplasmic and nuclear fractions and detected each protein in the fractions by using Western blotting. Consistent with the results using a confocal microscopy, endogenous and transfected OTT mainly localized in the nucleus (Fig. 4, *D* and *E*). Although endogenous and transfected BSAC predominantly localized in the cytoplasm and the small population of BSAC localized in the nucleus, transfected OTT-BSAC exclusively localized in the nucleus. Collectively, OTT fusion to BSAC drastically changed the subcellular localization of BSAC. This might be one of the molecular mechanisms underlying the aberrant up-regulation of OTT-BSAC-dependent transcriptional activity.

OTT Interacts with HDAC3—A previous study has shown that SHARP interacts with HDACs, SMRT, and N-CoR and acts as a transcriptional repressor (5). OTT has a structural similarity to SHARP (5, 6), prompting us to test whether OTT interacts with HDACs. We transiently transfected HEK293 cells with Myc-OTT along with FLAG-HDAC1, -2, or -3. The lysates were immunoprecipitated with anti-Myc antibody, and co-immunoprecipitated HDACs were detected by anti-FLAG antibody. HDAC3, but not HDAC1 or HDAC2, was specifically co-immunoprecipitated with OTT (Fig. 5*A*). In contrast, BSAC could not bind to HDAC3. A reciprocal immunoprecipitation experiment showed that OTT was also co-immunoprecipitated with HDAC3 (Fig. 5*A*). On the other hand, OTT did not interact with HDAC6, a member of the class II HDAC family (data

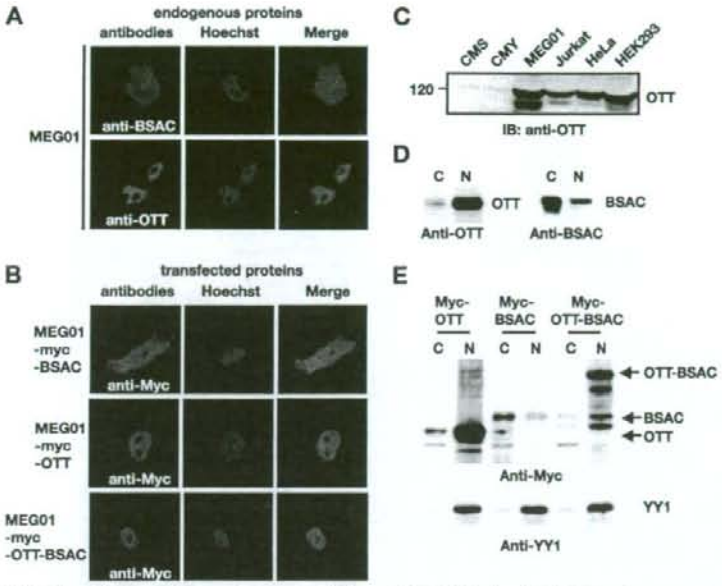

FIGURE 4. **Signal-independent nuclear accumulation of OTT-BSAC.** *A* and *B*, MEG-01 cells were untransfected (*A*) or transfected (*B*) with Myc-BSAC, Myc-OTT, or Myc-OTT-BSAC. Then the cells were stained with anti-BSAC (*A*), anti-OTT (*A*), or anti-Myc (*B*) antibodies and analyzed by a confocal microscopy. The nuclei were stained with Hoechst 33258 (*blue*) and the merged images are represented at the *right*. *C*, expression of OTT in various cell lines. Expression levels of endogenous OTT were analyzed by immunoblotting (*IB*) with anti-OTT antibody. The relative molecular mass (kDa) is indicated at the *left*. *D*, subcellular fractionation of endogenous OTT and BSAC in MEG-01 cells. Subcellular fractionation was performed as described under "Experimental Procedures," and equal amounts of proteins were subjected to SDS-PAGE. The expression levels of OTT and BSAC were analyzed by immunoblotting with anti-OTT and anti-BSAC antibodies, respectively. *C* and *N* indicate the cytosolic and nuclear fractions, respectively. *E*, subcellular localization of transfected Myc-OTT, Myc-BSAC, and Myc-OTT-BSAC. MEG-01 cells were transfected with the indicated vectors, and the subcellular fractionation and SDS-PAGE were performed as in *D*. Expression levels of transfected proteins in each fraction were analyzed by immunoblotting with anti-Myc antibody (*top panel*). The equal loading of the nuclear extracts was verified by immunoblotting with anti-YY1 antibody (*bottom panel*).

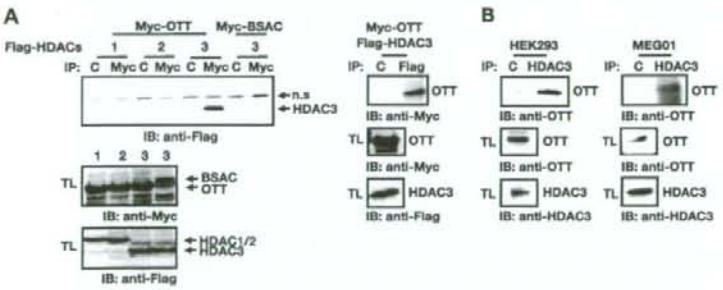

FIGURE 5. **OTT physically interacts with HDAC3.** *A*, OTT interacts with HDAC3, but not HDAC1 or HDAC2. HEK293 cells were transfected with the indicated expression vectors. After immunoprecipitation (*IP*) with control (*lane C*), anti-Myc, or anti-FLAG antibodies, co-immunoprecipitated proteins were detected by immunoblotting (*IB*) with anti-FLAG or anti-Myc antibodies (*top panel*). Expression levels of the transfected proteins in the total lysates (*TL*) were analyzed by immunoblotting with anti-Myc or anti-FLAG antibodies, respectively (*middle* and *bottom panels*). The *numbers 1*, *2*, and *3* indicate HDAC1, HDAC2, and HDAC3, respectively. *B*, endogenous interaction of OTT with HDAC3 in HEK293 and MEG-01 cells. After immunoprecipitation with control (*lane C*) or anti-HDAC3 antibodies, co-immunoprecipitated OTT was detected by immunoblotting with anti-OTT antibody (*top panels*). Expression levels of endogenous OTT and HDAC3 in the total lysates were analyzed by immunoblotting with anti-OTT and HDAC3 antibodies, respectively (*middle* and *bottom panels*).

not shown). To confirm the interaction of OTT with HDAC3 under more physiological conditions, we immunoprecipitated the lysates from HEK293 and MEG-01 cells with anti-HDAC3 antibody, and then co-immunoprecipitated OTT was detected with anti-OTT antibody. Anti-HDAC3, but not control antibody efficiently co-immunoprecipitated endogenous OTT (Fig. 5*B*). Collectively, these results indicate that OTT physically interacts with HDAC3 *in vivo*.

It is well known that HDAC3 is a component of a large nuclear corepressor complex including Sin3A, N-CoR, and SMRT. We next tried to detect interaction of OTT with Sin3A, N-CoR, and SMRT; however, under our experimental conditions, we could not detect direct interaction of OTT with either of them (data not shown). Therefore, future study will be required to address whether OTT might be a component of the nuclear corepressor complex.

Domain Mapping of OTT and HDAC3 for Their Interaction—We next delineated the regions of HDAC3 and OTT responsible for their interaction. Co-immunoprecipitation experiments using deletion mutants of HDAC3 revealed that N-terminal 307 amino acids were sufficient for binding to OTT (Fig. 6, *A* and *B*). Because the expression levels of HDAC3ΔN were consistently very low because of an increase in sensitivity to degradation of the transfected HDAC3ΔN in the cells, we could not formally exclude the possibility that HDAC3ΔN may also mediate the interaction of HDAC3 with OTT.

To determine the binding region of OTT to HDAC3, we constructed a series of deletion mutants of OTT and expressed them as fusion proteins with the DNA-binding domain of GAL4 (Fig. 6*C*). Although a region containing 609–730 amino acids could not bind to HDAC3, the N-terminal region containing three RNA recognition motifs and the C-terminal SPOC domains independently bound to HDAC3 (Fig. 6*D*), indicating that OTT interacts with HDAC3 via multiple regions.

OTT-BSAC Does Not Interact with HDAC3—We next investigated whether BSAC fusion to OTT could affect the ability to

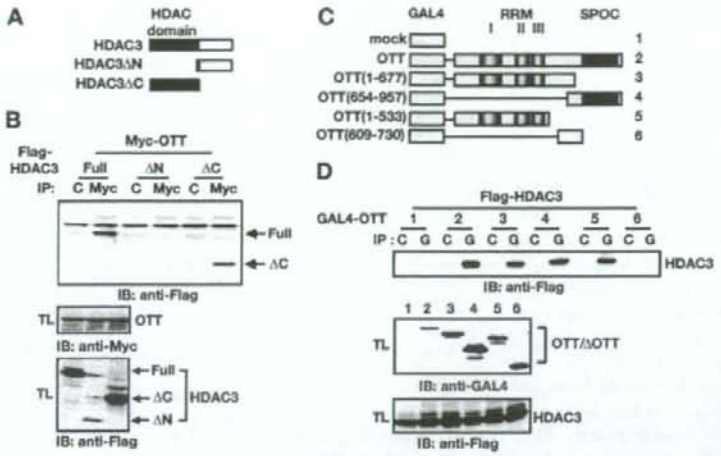

FIGURE 6. **Domain mapping of HDAC3 and OTT for their interaction.** *A*, schematic diagrams of deletion mutants of HDAC3. *B*, N-terminal HDAC domain is responsible for the binding to OTT. HEK293 cells were transfected with the indicated mutants of HDAC3 along with Myc-OTT. After immunoprecipitation (*IP*) with control (*lane C*) or anti-Myc antibodies, co-immunoprecipitated proteins were detected by immunoblotting (*IB*) with anti-FLAG antibody (*top panel*). Expression levels of transfected proteins (*TL*) were analyzed as in Fig. 5*A* (*middle* and *bottom panels*). *C*, schematic diagrams of deletion mutants of OTT fused to the DNA-binding domain of GAL4. *D*, OTT interacts with HDAC3 via multiple regions. HEK293 cells were transfected with the indicated mutants of GAL4-OTT along with FLAG-HDAC3. After immunoprecipitation with control (*lanes C*) or anti-GAL4 (*lanes G*) antibodies, co-immunoprecipitated proteins were detected by immunoblotting with anti-FLAG antibody (*top panel*). Expression levels of transfected proteins (*TL*) were analyzed as in Fig. 5*A* (*middle* and *bottom panels*). The *numbers* indicate each mutant of GAL4-OTT described as in *C*.

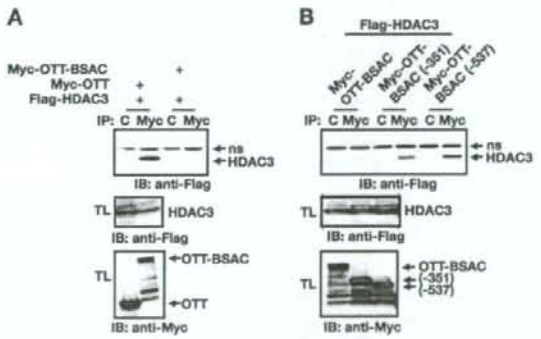

FIGURE 7. **BSAC fusion to OTT disrupts the interaction of OTT with HDAC3.** *A*, HEK293 cells were transfected with FLAG-HDAC3 along with Myc-OTT or Myc-OTT-BSAC. After immunoprecipitation (*IP*) with control (*lane C*) or anti-Myc antibodies, co-immunoprecipitated proteins were detected by immunoblotting (*IB*) with anti-FLAG antibody (*top panel*). Expression levels of the transfected proteins in the total lysates (*TL*) were analyzed as in Fig. 5*A* (*middle* and *bottom panels*). *ns* indicates nonspecific bands. *B*, HEK293 cells were transfected with FLAG-HDAC3 along with the indicated deletion mutants of Myc-OTT-BSAC. Immunoprecipitation and Western blotting were performed as in Fig. 5*A*.

interact with HDAC3. Interestingly, OTT-BSAC lost the ability to interact with HDAC3 (Fig. 7*A*). Given that the domain structure of OTT is preserved in OTT-BSAC, this suggests that some region of BSAC could inhibit the interaction of OTT with HDAC3. To determine the inhibitory region, we constructed C-terminal deletion mutants of OTT-BSAC (Fig. 7*B*). Deletion of C-terminal 351 amino acids containing the TA domain of OTT-BSAC restored the binding to HDAC3, suggesting that the C-terminal TA domain inhibits the binding of HDAC3 to OTT.

DISCUSSION

In the present study, we have shown that a fusion protein OTT-BSAC exhibited strong transcriptional activity to various promoters containing the YY1-binding sequences. Although BSAC predominantly localized in the cytoplasm, OTT-BSAC exclusively localized in the nucleus. This signal-independent nuclear accumulation of OTT-BSAC might contribute to a significant enhancement of transcriptional activity. Moreover, OTT interacted with HDAC3, but this interaction was abolished in OTT-BSAC. Given that OTT negatively regulates the myeloid and megakaryocyte expansion (26, 27), the loss of suppressor function of OTT along with aberrant up-regulation of BSAC-dependent transactivation caused by the fusion may culminate in the development of leukemia.

We and others have previously reported that BSAC activates the promoters containing CArG boxes through association with SRF (9–11). However, given that CArG boxes are found in the promoters of many immediate early genes or muscle-specific genes, it is unlikely that CArG box-dependent transcriptional activity of BSAC directly links to the development of leukemia. Thus, we surmised that OTT-BSAC activates a promoter containing a sequence other than the CArG box(es). We found that OTT-BSAC activated the *GPVI* promoter through YY1-binding sequences. This conclusion is supported by the following results. First, OTT-BSAC-mediated transcriptional activity was abolished on the *GPVI* promoters, in which the YY1-binding sequences were mutated (Fig. 2*B*). Second, YY1 bound to this site using EMSAs (Fig. 2*C*). Third, ChIP assays revealed that endogenous YY1 bound to the *GPVI* promoter (Fig. 2*D*). However, we could not detect the recruitment of transfected OTT-BSAC to the promoter of *GPVI* using ChIP assays under our experimental conditions (Fig. 2*E*). It is reasonable to speculate that only small populations of transfected OTT-BSAC might be recruited to the promoter; therefore such recruitment might be under the detection levels.

Although the present study has shown that OTT-BSAC activates the *GPVI* and other promoters containing the YY1-binding sequences, it remains unclear which transcriptional factor(s) is essential for OTT-BSAC-mediated transcriptional activation. Although overexpression of YY1 attenuated OTT-BSAC-dependent transcriptional activation (Fig. 3*A*), knockdown of YY1 using siRNA did not impair its transcriptional activity (Fig. 3*D*). Given that we could not detect the interaction of YY1 with OTT-BSAC (data not shown), OTT-BSAC might

be recruited to the YY1-binding motif through interaction with a transcription factor other than YY1. Intriguingly, YY2, a member of the YY1 family, has been shown to bind to the consensus binding sequences similar to YY1 (28); YY2 may recruit OTT-BSAC to the *GPVI* promoter. Further study will be required to address this possibility.

A previous study has shown that persistent expression of YY1 in 3DO cells after differentiation signal could perturb the granulocyte differentiation (18). Moreover, up-regulation of *YY1* mRNA is frequently observed in some patients of acute myeloid leukemia (18). These results indicate an intimate link between deregulation of YY1 and leukemia. Together, OTT-BSAC might modulate YY1- and/or YY1-related transcriptional factor-dependent transcription, culminating in the development of leukemia.

Another important finding of this study is that OTT fusion to the N terminus of BSAC resulted in signal-independent nuclear accumulation of OTT-BSAC. A previous study has shown that nuclear translocation of BSAC is tightly regulated by the Rho-actin signaling pathway (12). Consistently, under unstimulated conditions, endogenous BSAC predominantly localized in the cytoplasm (Fig. 4). These results suggest that transcriptional activity of BSAC is at least partly regulated by its subcellular localization. This might well explain the reason why OTT-BSAC shows stronger transcriptional activity than BSAC. However, the mechanism by which OTT-BSAC constitutively accumulates in the nucleus remains to be solved in this study. One possible scenario is that the nuclear localization signal(s) of OTT might dominate over the cytoplasmic retention signal(s) of BSAC. Although BSAC has its own nuclear localization signals in the basic domain, N-terminal RPEL motifs are considered to sequestrate BSAC to the cytoplasm via interaction with G actin under unstimulated conditions (12). Therefore, OTT might disrupt such inhibition, resulting in constitutive nuclear translocation of OTT-BSAC.

A recent study has shown that deletion of *OTT* gene results in megakaryocytic expansion (27). In addition, knockdown of *OTT/RBM15* gene using RNA interference promotes myeloid differentiation (26), suggesting an inhibitory role for OTT in myeloid and megakaryocyte development. These results are consistent with our present study, in which OTT might act as a transcriptional repressor via interaction with HDAC3 (Fig. 6). Given that this transcriptional repressor activity of OTT might be abolished in OTT-BSAC, the loss of OTT-mediated suppressor function of OTT-BSAC along with aberrant up-regulation of BSAC-dependent transcriptional activity might synergistically contribute to the development of leukemia.

Acknowledgments—We thank Drs. Don Ayer, Edward Seto, Stuart Schreiber, Jiemin Wang, A. Gregory Materal, Ron M. Evans, the Kazusa DNA Institute, Takeyuki Sato, and Masao Seto for providing reagents and cell lines. We also thank Drs. Alan B. Cantor, Jean-Pierre Bourquin, Yuriko Suzuki, Tatsuo Fukagawa, Mitsuru Matsumoto, and Mikiko Chihara-Siomi for helpful discussion.

REFERENCES

1. Struhl, K. (1998) *Genes Dev.* **12,** 599–606
2. Ng, H. H., and Bird, A. (2000) *Trends Biochem. Sci* **25,** 121–126
3. Yang, X. J., and Gregoire, S. (2005) *Mol. Cell. Biol.* **25,** 2873–2884
4. Jepsen, K., and Rosenfeld, M. G. (2002) *J. Cell Sci.* **115,** 689–698
5. Shi, Y., Downes, M., Xie, W., Kao, H. Y., Ordentlich, P., Tsai, C. C., Hon, M., and Evans, R. M. (2001) *Genes Dev.* **15,** 1140–1151
6. Ariyoshi, M., and Schwabe, J. W. (2003) *Genes Dev.* **17,** 1909–1920
7. Mercher, T., Coniat, M. B., Monni, R., Mauchauffe, M., Khac, F. N., Gressin, L., Mugneret, F., Leblanc, T., Dastugue, N., Berger, R., and Bernard, O. A. (2001) *Proc. Natl. Acad. Sci. U. S. A.* **98,** 5776–5779
8. Ma, Z., Morris, S. W., Valentine, V., Li, M., Herbrick, J. A., Cui, X., Bouman, D., Li, Y., Mehta, P. K., Nizetic, D., Kaneko, Y., Chan, G. C., Chan, L. C., Squire, J., Scherer, S. W., and Hitzler, J. K. (2001) *Nat. Genet.* **28,** 220–221
9. Sasazuki, T., Sawada, T., Sakon, S., Kitamura, T., Kishi, T., Okazaki, T., Katano, M., Tanaka, M., Watanabe, M., Yagita, H., Okumura, K., and Nakano, H. (2002) *J. Biol. Chem.* **277,** 28853–28860
10. Wang, D. Z., Li, S., Hockemeyer, D., Sutherland, L., Wang, Z., Schratt, G., Richardson, J. A., Nordheim, A., and Olson, E. N. (2002) *Proc. Natl. Acad. Sci. U. S. A.* **99,** 14855–14860
11. Cen, B., Selvaraj, A., Burgess, R. C., Hitzler, J. K., Ma, Z., Morris, S. W., and Prywes, R. (2003) *Mol. Cell. Biol.* **23,** 6597–6608
12. Miralles, F., Posern, G., Zaromytidou, A. I., and Treisman, R. (2003) *Cell* **113,** 329–342
13. Li, S., Chang, S., Qi, X., Richardson, J. A., and Olson, E. N. (2006) *Mol. Cell. Biol.* **26,** 5797–5808
14. Sun, Y., Boyd, K., Xu, W., Ma, J., Jackson, C. W., Fu, A., Shillingford, J. M., Robinson, G. W., Hennighausen, L., Hitzler, J. K., Ma, Z., and Morris, S. W. (2006) *Mol. Cell. Biol.* **26,** 5809–5826
15. Shi, Y., Lee, J. S., and Galvin, K. M. (1997) *Biochim. Biophys. Acta* **1332,** 49–66
16. Thomas, M. J., and Seto, E. (1999) *Gene (Amst.)* **236,** 197–208
17. Donohoe, M. E., Zhang, X., McGinnis, L., Biggers, J., Li, E., and Shi, Y. (1999) *Mol. Cell. Biol.* **19,** 7237–7244
18. Erkeland, S. J., Valkhof, M., Heijmans-Antonissen, C., Delwel, R., Valk, P. J., Hermans, M. H., and Touw, I. P. (2003) *Blood* **101,** 1111–1117
19. Ogura, M., Morishima, Y., Ohno, R., Kato, Y., Hirabayashi, N., Nagura, H., and Saito, H. (1985) *Blood* **66,** 1384–1392
20. Nishiyama, C., Hasegawa, M., Nishiyama, M., Takahashi, K., Akizawa, Y., Yokota, T., Okumura, K., Ogawa, H., and Ra, C. (2002) *J. Immunol.* **168,** 4546–4552
21. Muraoka, O., Kaisho, T., Tanabe, M., and Hirano, T. (1993) *Immunol. Lett.* **37,** 159–165
22. Nakano, H., Shindo, M., Sakon, S., Nishinaka, S., Mihara, M., Yagita, H., and Okumura, K. (1998) *Proc. Natl. Acad. Sci. U. S. A.* **95,** 3537–3542
23. Kanada, S., Nakano, N., Potaczek, D. P., Maeda, K., Shimokawa, N., Niwa, Y., Fukai, T., Sanak, M., Szczeklik, A., Yagita, H., Okumura, K., Ogawa, H., and Nishiyama, C. (2008) *J. Immunol.* **180,** 8204–8210
24. Holmes, M. L., Bartle, N., Eisbacher, M., and Chong, B. H. (2002) *J. Biol. Chem.* **277,** 48333–48341
25. Wang, D., Chang, P. S., Wang, Z., Sutherland, L., Richardson, J. A., Small, E., Krieg, P. A., and Olson, E. N. (2001) *Cell* **105,** 851–862
26. Ma, X., Renda, M. J., Wang, L., Cheng, E. C., Niu, C., Morris, S. W., Chi, A. S., and Krause, D. S. (2007) *Mol. Cell. Biol.* **27,** 3056–3064
27. Raffel, G. D., Mercher, T., Shigematsu, H., Williams, I. R., Cullen, D. E., Akashi, K., Bernard, O. A., and Gilliland, D. G. (2007) *Proc. Natl. Acad. Sci. U. S. A.* **104,** 6001–6006
28. Nguyen, N., Zhang, X., Olashaw, N., and Seto, E. (2004) *J. Biol. Chem.* **279,** 25927–25934

Laboratory Investigation (2008) 88, 652–663

Decoy oligodeoxynucleotide targeting activator protein-1 (AP-1) attenuates intestinal inflammation in murine experimental colitis

Ichiro Moriyama[1], Shunji Ishihara[1], M Azharul Karim Rumi[2], MD Monowar Aziz[1], Yoshiyuki Mishima[1], Naoki Oshima[1], Chikara Kadota[1], Yasunori Kadowaki[1], Yuji Amano[3] and Yoshikazu Kinoshita[1]

Various therapies are used for inflammatory bowel diseases (IBD), though none seem to be extremely effective. AP-1 is a major transcription factor that upregulates genes involved in immune and proinflammatory responses. We investigated decoy oligodeoxynucleotide (ODN) targeting AP-1 to prevent dextran sulfate sodium (DSS)-induced colitis in mice. Functional efficacies of synthetic decoy and scrambled ODNs were evaluated *in vitro* by a reporter gene luciferase assay and measuring flagellin-induced IL-8 expression by HCT-15 cells transfected with ODNs. Experimental colitis was induced in mice with a 2.5% DSS solution in drinking water for 7 days, and decoy or scrambled ODNs were intraperitoneally injected from days 2 to 5. Colitis was assessed by weight loss, colon length, histopathology, and detection of myeloperoxidase (MPO), IL-1β, and TNF-α in colon tissue. Therapeutic effects of AP-1 and NF-κB decoy ODNs were compared. Transfection of AP-1 decoy ODN inhibited AP-1 transcriptional activity in reporter assays and flagellin-induced IL-8 production *in vitro*. In mice, AP-1 decoy ODN, but not scrambled ODN, significantly inhibited weight loss, colon shortening, and histological inflammation induced by DSS. Further, AP-1 decoy ODN decreased MPO, IL-1β, and TNF-α in colonic tissue of mice with DSS-induced colitis. The AP-1 decoy therapeutic effect was comparable to that of NF-κB decoy ODN, which also significantly decreased intestinal inflammation. Double-strand decoy ODN targeting AP-1 effectively attenuated intestinal inflammation associated with experimental colitis in mice, indicating the potential of targeting proinflammatory transcription factors in new therapies for IBD.

Laboratory Investigation (2008) **88,** 652–663; doi:10.1038/labinvest.2008.38; published online 5 May 2008

KEYWORDS: decoy oligodeoxynucleotide; AP-1; NF-κB; inflammatory bowel disease; experimental colitis

Ulcerative colitis (UC) and Crohn's disease (CD) are two major forms of inflammatory bowel diseases (IBD), which are characterized by chronic intestinal immune-mediated disorders of unknown etiology.[1–5] In sites of intestinal inflammation, granulocytes and macrophages produce high levels of pro-inflammatory cytokines, including interleukin (IL)-1β, IL-6, and tumor necrosis factor (TNF)-α, which are directly involved in the pathogenesis of IBD.[1–3,6–9] Although several kinds of therapeutic strategies are used for IBD, none have been found to be totally effective. Conventional therapies for IBD focus on suppression and control of inflammation using 5-aminosalicylates, corticosteroids, and immune-modulating drugs, such as azathioprine and mercaptopurine.[10–14] On the other hand, recently developed novel cytokine antagonist therapies targeting TNF-α and IL-6 have been found to be quite effective in certain IBD patients.[15–18] Such molecular targeted inhibition of inflammatory processes may provide better therapeutic options for IBD and studies have been conducted to evaluate new innovative approaches.

Gene expression in a variety of biological conditions is initiated and regulated at the transcriptional level by interactions between specialized nuclear proteins, termed transcription factors, and promoter regions containing DNA elements that exhibit specific nucleotide sequences.[19,20] The transcription factor-activated protein-1 (AP-1) is a dimeric complex of basic region-leucine zipper proteins, and consists of heterodimers or homodimers of the Jun, Fos, and ATF

[1]Department of Internal Medicine II, Shimane University School of Medicine, Shimane, Japan; [2]Department of Pathology and Laboratory of Medicine, University of Kansas Medical Center, Kansas City, Kansas, USA and [3]Division of Gastrointestinal Endoscopy, Shimane University Hospital, Shimane, Japan
Correspondence: Dr S Ishihara, MD, PhD, Department of Internal Medicine II, Shimane Medical University, 89-1, Enya-cho, Izumo, Shimane 693-8501, Japan.
E-mail: si360405@med.shimane-u.ac.jp

Received 09 October 2007; revised 28 February 2008; accepted 28 February 2008

families.[21–23] AP-1 is modulated by interactions with other transcriptional regulators and is further controlled by upstream kinases that link AP-1 to various signal transduction pathways.[24–26] AP-1 binds to specific DNA sequences present in a large number of genes that regulate inflammation, cellular growth, and differentiation.[21,27–30] Several agents that suppress AP-1 activation have been shown to inhibit inflammation and tumorigenesis. Recent studies have demonstrated that AP-1 is one of the key transcription factors that upregulate genes involved in immune as well as proinflammatory responses during the pathogenesis of IBD, suggesting that AP-1 may be an ideal target for the development of new therapeutic options for IBD.[31,32]

A decoy strategy that employs a synthetic double-stranded (ds) oligonucleotide (ODN) to competitively inhibit the binding of transcription factors to promoter regions of their target genes has emerged as a useful tool in a new class of antigene therapies presented in recent years.[33,34] It has been reported that a decoy ODN targeted at the transcription factor nuclear factor (NF)-κB, which plays an essential role in the regulation of a large number of genes involved in immune and inflammatory response, can exert potent immunosuppressive effects with certain inflammatory diseases.[35–37] Although the effects of AP-1 decoy ODN have been recently studied in several experimental disease models,[38–40] nothing is known regarding its therapeutic potential in gastrointestinal inflammation, including IBD.

In the present study, we investigated the anti-inflammatory effects of AP-1 decoy ODN in dextran sulfate sodium (DSS)-induced experimental murine colitis and compared its therapeutic potential to that of NF-κB decoy ODN. AP-1 decoy ODN treatment markedly inhibited colonic inflammation during DSS-induced colitis, suggesting that additional approaches with targeted inhibition of the transcription factor AP-1 including use of decoy ODN may contribute to development of a new therapeutic strategy for IBD.

MATERIALS AND METHODS

Synthesis of Double-Strand ODN

Synthetic ds decoy ODN was obtained as an HPLC-purified product from Hokkaido System Science (Sapporo, Japan). The ds decoy ODN was generated by annealing equimolar amounts of single-stranded sense and antisense phosphorothioate-modified ODN containing consensus AP-1 or NF-κB-binding sequences. Scrambled ds ODN samples were also generated as experimental controls for each decoy ODN. The phosphorothioate ODN used in this study had the following sequences (consensus sequences are underlined):

Decoy ODN for AP-1;
5′-TGTCTGACTCATGTC-3′
3′-ACAGACTGAGTACAG-5′
Scrambled ODN for AP-1;
5′-TGTCTCTCTGATGTC-3′
3′-ACAGAGAGACTACAG-5′
Decoy ODN for NF-κB;
5′-CCTTGAAGGGATTTCCCTCC-3′
3′-GGAACTTCCCTAAAGGGAGG-5′
Scrambled ODN for NF-κB;
5′-TTGCCGTACCTGACTTAGCC-3′
3′-AACGGCATGGACTGAATCGG-5′

Cell Line and Culture Condition

The human cell line HCT-15 was obtained from American Type Culture Collection (ATCC, Manassas, MD, USA). HCT-15 cells were grown in RPMI-1640 (ICN Biomedicals, Aurora, OH, USA), supplemented with 10% fetal bovine serum (FBS; ICN Biomedicals) and penicillin-streptomycin-amphotericin B (GIBCO BRL), and maintained at 37°C in an incubator with 5% CO_2 and constant humidity.

Transfections of Decoy and Scrambled ODN and Transfection Efficiency

HCT-15 cells were cultured in 24-well plates (5×10^4 cells per well) and transfected with FITC-labeled decoy or scrambled ODN (0.25 μg per well) using Lipofectamine 2000 (Invitrogen, NY, USA), according to the manufacturer's protocol. Twenty-four hours after transfection, efficiency was assessed by fluorescence microscopy (Olympus, Tokyo, Japan) and flow cytometry. For flow cytometry, cells were harvested with trypsin-EDTA treatment, washed five times with cold PBS, and analyzed using an EPICS XL (Beckman Coulter, Tokyo, Japan), in which 10 000 events were counted for each condition and analyzed using EXPO32™ software.

Functional Efficiency of Decoy AP-1 and NF-κB ODNs

The efficiency of the decoy ODNs to mediate the inhibition of AP-1 or NF-κB-induced transcription activity was initially evaluated *in vitro* using a reporter gene luciferase assay. Reporter vectors were constructed by cloning AP-1 or NF-κB-binding consensus DNA elements into the promoter sequences, in which pNF-κB-Luc contained five copies of the NF-κB element 5′-TGGGGACTTTCCGC-3′ cloned upstream to the minimal TATA promoter (Stratagene Cloning Systems, La Jolla, CA, USA) and pAP-1-Luc contained five copies in a tandem repeat of the AP-1-binding site (TGACTAA), followed by cloning of the minimal TATA promoter into a pGL3-Basic vector (Promega, Madison, WI, USA). As an internal control for the dual luciferase assay, a pRL-TATA vector was constructed by cloning the minimal TATA promoter into a pRL-null vector (Promega) upstream of the renilla luciferase coding sequence. HCT-15 cells were cultured in 24-well plates (5×10^4 cells per well) and transfected with various concentrations of decoy or scrambled ODN, 0.1 μg of pNF-κB-Luc or pAP-1-Luc, and 0.02 μg of pRL-TATA per well using Lipofectamine 2000 transfection reagent (Invitrogen). Twenty-four hours after transfection, cells were stimulated with *salmonella* flagellin (0.1 μg/ml, Invitrogen, San Diego, USA), a ligand for toll-like receptor (TLR)-5, for 12 h. The cell lysates were then used for measurement of firefly and renilla luciferase activities with a PicaGene Dual

luciferase kit (Toyoinki, Tokyo, Japan). As a control, the effects of various concentrations of decoy or scrambled ODN on transcriptional activities in cultured cells without flagellin stimulation were also evaluated.

In addition to the reporter gene assays, the functional efficacy of AP-1 or NF-κB decoy ODN on AP-1 or NF-κB-induced endogenous proinflammatory gene expression was evaluated by their effects on flagellin-induced IL-8 expression by HCT-15 cells. Cells were grown in 24-well plates, transfected with various concentrations of decoy or scrambled ODNs, and stimulated with flagellin (0.1 μg/ml) for 24 h. Then, cell culture supernatants were collected for measurement of IL-8 using an enzyme immunoassay (EIA) (R&D Systems, Uden, Minneapolis, USA). For quantitative determination of IL-8 mRNA expression, total RNA was isolated using a guanidine thiocyanate-phenol-chloroform method (Isogen; Nippon Gene Co., Tokyo, Japan). From each sample, 1 μg of RNA was reverse transcribed into cDNA using the random primer from an affinity script QPCR cDNA synthesis kit (Stratagene, La Jolla, CA). Real-Time PCR was carried out in a total reaction volume of 30 μl using power SYBR Green PCR master mix (Applied Biosystem, Warrington, UK) and run on an ABI Prism 7000 Sequence Detection System (Applied Biosystems, Foster City, USA). The primers used for transcript confirmation were as follows: IL-8 (sense), 5′-TGTGTGTAAACATGACTTCCAAGCT-3′; IL-8 (anti-sense), 5′-TTAGCACTCCTTGGCAAAACTG-3′, and GAPDH (sense), 5′-CCACATCGCTCAGACACCAT-3′; and GAPDH (antisense), 5′-TGACCAGGCGCCCAATA-3′. Finally, the results were expressed as the ratio of mean quantity of IL-8 to corresponding GAPDH for each sample. As a control, the effects of various concentrations of decoy or scrambled ODN on IL-8 expression in cultured cells without flagellin stimulation were also evaluated.

Effects of Decoy AP-1 and NF-κB ODNs on TNF-α-Mediated IL-8 Production *In Vitro*

Tumor necrosis factor-α, which regulates various inflammatory mediators, is considered to be one of the key molecules for the pathogenesis of IBD.[41] Because IL-8 is one of the major pro-inflammatory genes mediated by TNF-α stimulation, the effects of decoy ODNs on IL-8 production in HCT-15 cells were examined. Cells were grown in 24-well plates, transfected with decoy or scrambled ODNs (0.5 μg/ml), and stimulated with flagellin (0.1 μg/ml) for 24 h. Then, cell culture supernatants were collected for measurement of IL-8 using an EIA. As a control, the effects of decoy or scrambled ODN on IL-8 production in cultured cells without flagellin stimulation were also evaluated.

Experimental Colitis and Decoy ODN Therapy Protocol

Seven-week-old specific pathogen-free male BALB/c mice (Nihon Clea, Tokyo, Japan) were studied after receiving approval from the Ethics Committee for Animal Experimentation of Shimane University. The animals were housed under constant environmental conditions with circadian light/dark cycles. After an initial adaptation period of 1 week, a DSS solution (2.5% w/v) was administered to the experimental animals as drinking water for 7 days to produce experimental colitis. The *in vivo* study protocol is shown in Figure 3a. AP-1 or NF-κB decoy ODN (0, 5, 20, 40 μg per mouse) or scrambled ODN (0, 5, 20, 40 μg per mouse) was intraperitoneally injected once a day from days 2 to 5 during the DSS-administration period using a hemagglutinating virus of Japan (HVJ)-liposome method, as described previously.[38] The body weight (BW) of each mouse was measured daily until euthanasia. As a control, the effects of scrambled or decoy ODNs (0, 5, 20, 40 μg per mouse) on BW changes in mice without DSS treatment were also evaluated. The experimental animals were killed on day 8 after the end of DSS-administration by an overdose of diethyl ether, and then the colons were dissected out and rinsed in cold PBS. After measuring the total length of the colon, it was divided into proximal, medial, and distal portions. For this study, only the distal colon was examined, since it is considered to be most vulnerable to DSS-induced colitis. Further, a segment of the distal colon was processed for histological examinations and another was preserved for protein extraction.

Histological Examination

The colonic specimens were formalin-fixed and embedded in paraffin blocks. For the histological examinations, 3-μm paraffin sections were stained with hematoxylin and eosin. Two histopathologists blinded to the treatment groups examined each colonic section independently, as described previously.[42] During each histological examination, three different parameters were estimated, severity of inflammation (based on polymorphonuclear neutrophil infiltration; 0–3: none, slight, moderate, severe), depth of injury (0–3: none, mucosal, mucosal and submucosal, transmural), and crypt damage (0–4: none, basal one-third damaged, basal two-thirds damaged, only surface epithelium intact, entire crypt and epithelium lost). The score for each parameter was multiplied by a factor reflecting the percentage of tissue involvement (× 1, 0–25%; × 2, 26–50%; × 3, 51–75%; × 4, 76–100%) and all values were added to a sum, in which the maximum possible score was 40.

Detection of IL-1β, TNF-α and Myeloperoxidase Activity in Colonic Tissues

IL-1β, TNF-α, and myeloperoxidase (MPO) are considered to be major inflammatory mediators involved in the pathogenesis of intestinal inflammation. In particular, IL-1β and TNF-α have been reported to be AP-1-target genes.[43,44] Therefore, expressions of IL-1β, TNFα, and MPO in colonic tissues were evaluated using an EIA and real-time PCR. Each distal colonic tissue sample was weighed, then after grinding by liquid nitrogen chilled mortar and pestles, it was completely lysed by syringing in ice cold 20 mM Tris, pH 7.6, containing 0.1% SDS, 1% Triton X-100, 1% deoxycholate,

100 μg/ml of the protease inhibitor PMSF, and a protease inhibitor cocktail (Sigma-Aldrich, St Louis, MO, USA). Tissue lysates were centrifuged at 20 000 × *g* for 20 min at 4°C, then the supernatants were collected and the protein concentration was estimated by the Bradford method (Bio-Rad, Hercules, CA, USA). IL-1β contents and MPO activity were measured using EIA kits for IL-1β (R&D Systems, Uden, Minneapolis, USA) and MPO (Hycult Biotechnology, The Netherlands). The expression of TNF-α in colonic tissues was examined by real-time PCR, as described above, using the following primers: sense, 5′-AGACCCTCACACTCAGATCA TCTTC-3′; anti-sense, 5′-TCCTCCACTTGGTGGTTTGC-3′.

Statistical Analysis

All data are expressed as the mean ± s.e.m. The values were compared using Student's *t*-test with Stat-View 4.0 software (Abacus Concepts Inc., USA). A *P*-value of <0.05 was considered significant.

RESULTS

Transfection Efficiency and Functional *In Vitro* Effects of Decoy ODNs Toward HCT-15 Cells

To investigate the *in vitro* effects of the decoy ODNs, the transfection efficiency of the FITC-labeled ODNs was initially assessed using fluorescence microscopy. Twenty-four hours after transfection of the labeled decoy or scrambled ODN, high levels of fluorescence activity were observed in both the cytoplasm and nuclei of a large number of cultured cells (Figure 1a). Flow cytometry was then performed to quantify the proportion of transfected cells. Prior to flow cytometry, harvested cells were carefully washed with PBS to avoid non-specific fluorescence activity from labeled ODNs on the cell surface. The results of flow cytometry revealed high positive rates (above 90%) of fluorescence activity in the cultured cells transfected with the labeled decoy or scrambled ODN (Figure 1b).

Next, we examined the *in vitro* effects of decoy ODNs on the transcriptional activities of AP-1 and NF-κB using a reporter gene luciferase assay. Twenty-four hours after the transfection of reporter constructs that contained AP-1 or NK-κB-specific elements in their promoters along with the corresponding decoy or scrambled ODN, the cells were stimulated with flagellin. The results of the luciferase assay are shown in Figure 2a. Transfection of decoy ODNs significantly inhibited the transcriptional activities of the AP-1 and NF-κB promoter constructs in the cells in a dose-dependent manner. Further, the real-time PCR and EIA results showed significant inhibitory effects on IL-8 mRNA expression and protein production by the HCT-15 cells transfected with decoy ODNs (Figure 2b and c). In contrast, transfection of scrambled and decoy ODNs did not show any influence on luciferase activities or IL-8 expression in cultured cells without flagellin stimulation.

As TNF-α regulates various pro-inflammatory genes, the effects of decoy ODNs on TNF-α-mediated IL-8 production were also examined *in vitro*, with the results shown in Figure 2d. Treatment with decoy ODNs significantly inhibited TNF-α-mediated IL-8 production in cultured cells.

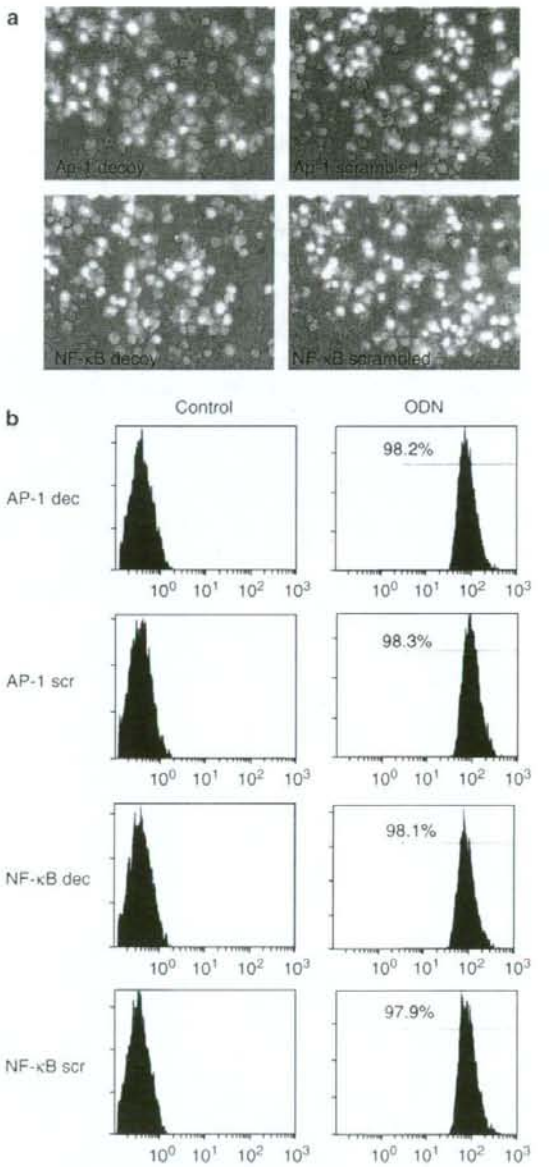

Figure 1 Transfection efficiency of decoy and scrambled ODNs in HCT-15 cells. Cells were cultured in 24-well plates and transfected with FITC-labeled decoy or scrambled ODN (0.25 μg/well). Twenty-four hours after transfection, efficiency was assessed by fluorescence microscopy (**a**) and flow cytometry (**b**). For flow cytometry, cells were harvested using trypsin-EDTA treatment, then washed five times with cold PBS and analyzed, with 10 000 events counted for each condition.

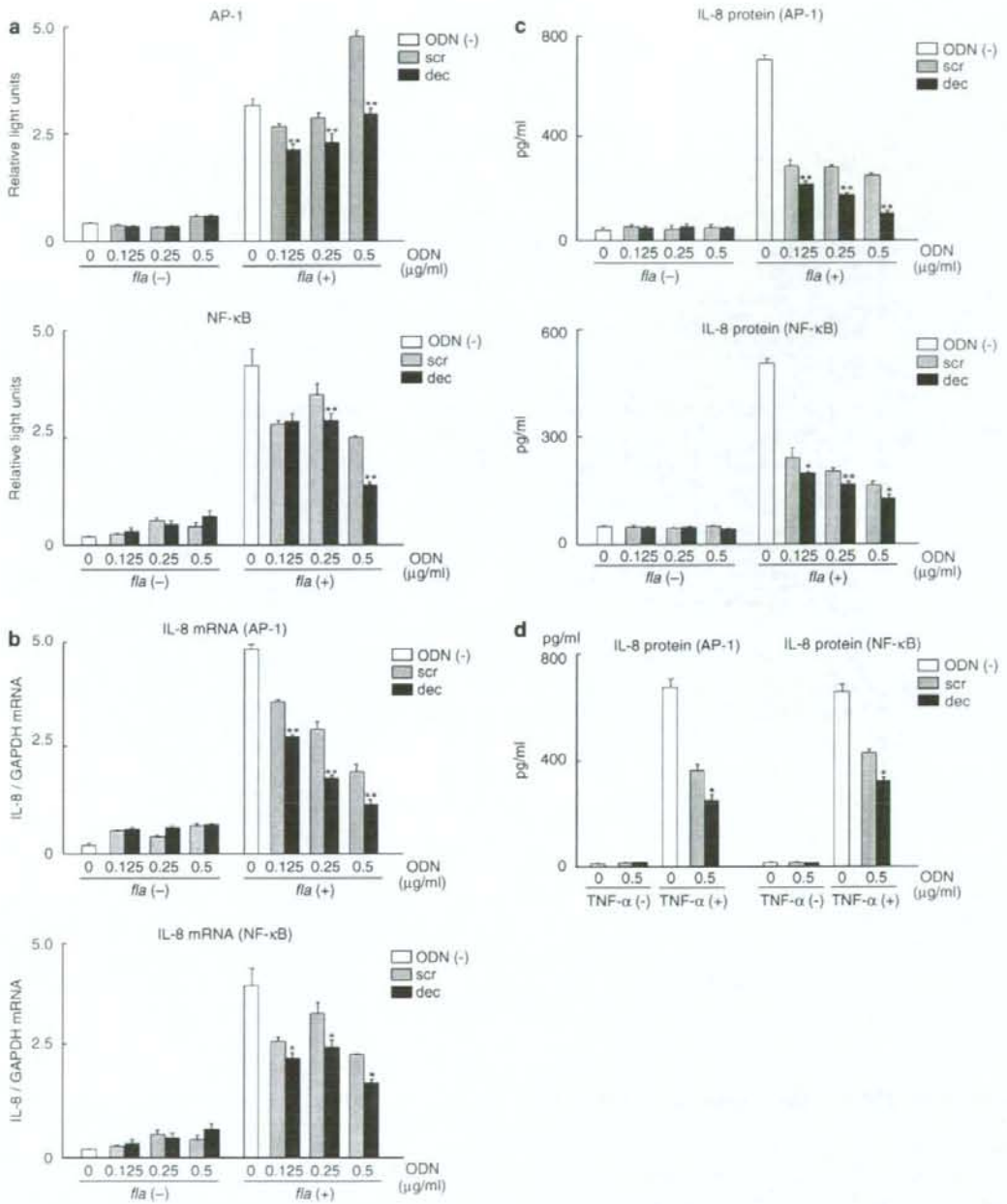

Figure 2 *In vitro* functional effects of decoy ODNs in HCT-15 cells. (**a**) The efficiency of decoy ODN-mediated inhibition of AP-1 and NF-κB-induced transcription activities was evaluated using a reporter gene luciferase assay. Cells were cultured in 24-well plates and transfected with various concentrations of decoy or scrambled ODNs, 0.1 μg of pNF-κB-Luc or pAP-1-Luc, and 0.02 μg of pRL-TATA per well. Twenty-four hours after transfection, cells were stimulated with or without flagellin (0.1 μg/ml) for 12 h, then cell lysates were used for the measurement of firefly and renilla luciferase activities. Data are expressed as relative light units obtained in dual-luciferase assays. (**b** and **c**) Functional efficacy of decoy ODNs on flagellin-induced IL-8 expression by HCT-15 cells transfected with ODNs. Cells were grown in 24-well plates, transfected with various concentrations of decoy or scrambled ODNs, and stimulated with or without flagellin (0.1 μg/ml) for 24 h. Cells and culture supernatants were used for quantitative determination of IL-8 mRNA expression and measurement of IL-8 protein content, respectively. (**d**) Effects of decoy AP-1 and NF-κB ODNs on TNF-α-mediated IL-8 production by HCT-15 cells transfected with ODNs. Cells were grown in 24-well plates, transfected with decoy or scrambled ODNs (0.5 μg/ml), and stimulated with flagellin (0.1 μg/ml) for 24 h. Cell culture supernatants were used for measurement of IL-8 using an EIA. Error bars indicate the standard error of mean values obtained from four independent experiments. $^{*}P<0.05$, $^{**}P<0.01$ *vs* scrambled ODN.

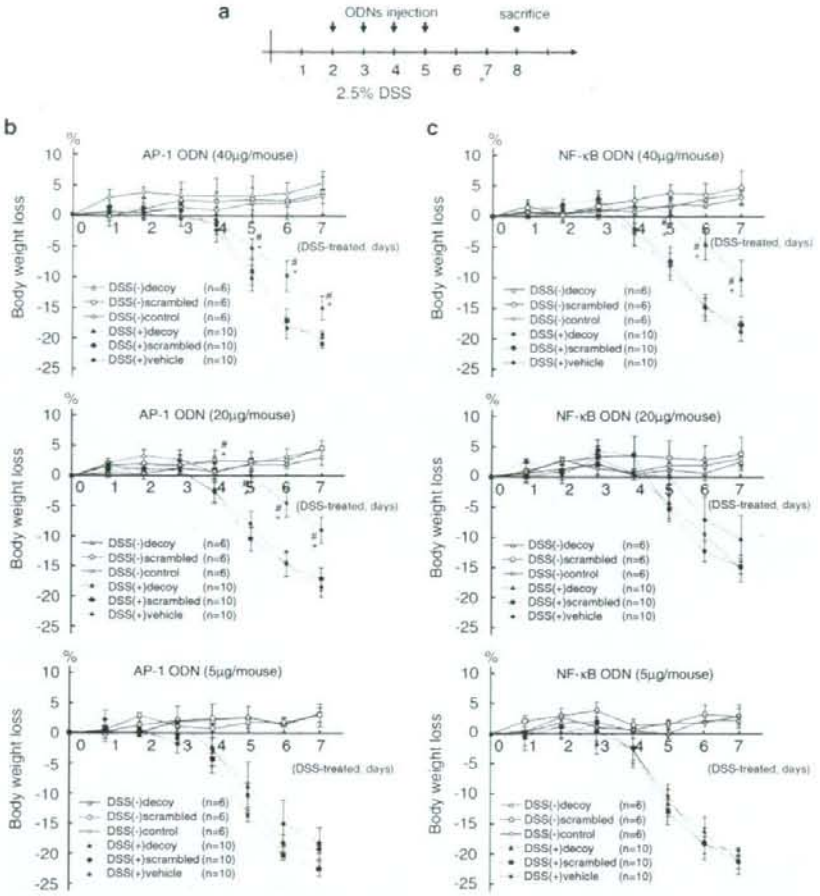

Figure 3 (**a**) Experimental colitis and decoy ODN therapy protocol. Experimental colitis models were established by administering a 2.5% DSS solution as drinking water for 7 days. Various concentrations of decoy or scrambled ODNs were intraperitoneally injected once a day from days 2 to 5 during the DSS-administration period using an HVJ-liposome method. As a control, the effects of the scrambled and decoy ODNs on BW changes in mice without DSS treatment were also evaluated. (**b** and **c**) Effects of AP-1 decoy and NF-κB decoy ODNs on BW changes in mice with or without DSS administration. Data are expressed as serial changes in percentage of BW during DSS administration. Error bars indicate the standard error of mean values obtained independently from 10 mice. $^{*}P<0.05$ *vs* DSS(+) scrambled ODN. $^{\#}P<0.05$ *vs* DSS(+) vehicle.

Effects of Decoy ODNs on BW Changes During Induction of DSS Colitis

As the decoy ODNs designed for this study had significant inhibitory effects on the transcriptional activities of AP-1 and NF-κB *in vitro*, we used them for further *in vivo* experiments. Experimental colitis models were established by administering a 2.5% DSS solution for 7 days. Each decoy, scrambled ODN, or the vehicle alone was intraperitoneally injected into mice with or without DSS administration once a day from days 2 to 5 during the experimental period (Figure 3a). In both the scrambled ODN and vehicle groups with DSS administration, BW loss of the mice commenced on day 4 and continued to day 7, whereas treatment with AP-1 decoy ODN (20, 40 μg per mouse) significantly inhibited BW loss from days 4 to 7 (Figure 3b). NF-κB decoy ODN (40 μg per mouse) also showed a significant inhibitory effect on BW loss from days 4 to 7, which was similar to the effect of AP-1 decoy ODN (Figure 3c). The BWs of mice injected with ODNs without DSS treatment were increased by about 5% on day 7, which was similar to the control mice. The doses that inhibited BW loss of DSS-treated mice most significantly were 20 μg for the AP-1 decoy ODN-injected group and 40 μg for the NF-κB decoy ODN-injected group. Colon length, histology, EIA, and real-time PCR findings for these groups are presented in Figures 4–6 and Table 1.

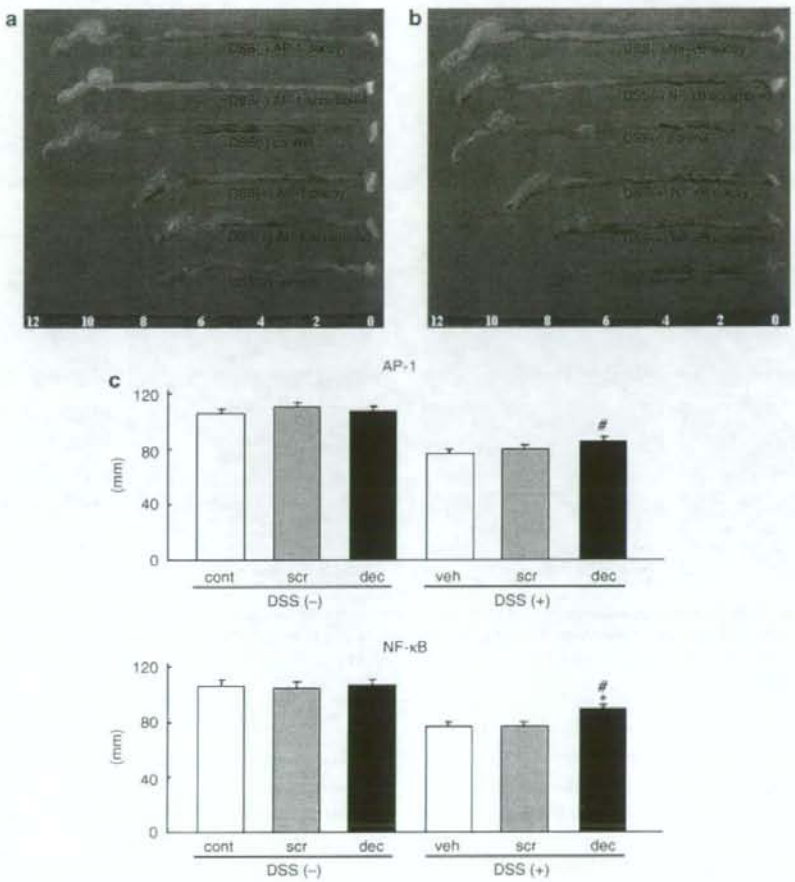

Figure 4 Effects of decoy ODNs on colon length in DSS-induced colitis. The experimental animals were euthanized on day 8, at the end of DSS administration. The total length of each colon dissected out from the mice was measured. (**a** and **b**) Representative images of colons dissected from DSS-non-treated and -treated mice following treatment with or without decoy and scrambled ODNs (AP-1: 20 μg/mouse, NF-κB: 40 μg/mouse). (**c**) Average total colon length in experimental groups treated with decoy ODN or scrambled ODN. Error bars indicate the s.e.m. values obtained independently from 10 mice. $^{*}P<0.05$ *vs* DSS(+) scrambled. $^{\#}P<0.05$ *vs* DSS(+) vehicle.

Effects of Decoy ODNs on Colon Length and Histology During Induction of DSS Colitis

The experimental animals were euthanized on day 8, at the end of DSS administration. Representative pictures of dissected colons are shown in Figure 4a and b. Treatment with AP-1 (20 μg per mouse) or NF-κB (40 μg per mouse) decoy ODNs, but not the scrambled ODNs or vehicle, significantly inhibited colon shortening induced by DSS administration (Figure 4c). Further, histological examinations showed that lamina propria infiltration by both polymorphonuclear and mononuclear cells as well as crypt epithelial damage were markedly decreased in the decoy ODN-treated mice (Figure 5a and b). All histological parameters as well as total histological score, as assessed by severity of inflammation, depth of injury, and crypt damage, in colon samples collected from decoy ODN-treated mice were significantly lower than those from scrambled ODN or vehicle-treated mice (Table 1).

Effects of Decoy ODNs on Expression of Pro-Inflammatory Cytokines and MPO Activity in Colonic Tissues

IL-1β, TNF-α, and MPO are major inflammatory mediators in the pathogenesis of IBD. As our histological examinations showed potent inhibitory effects on experimental colitis, we also evaluated the expression of pro-inflammatory cytokines and MPO activity in distal colon samples using an EIA and real-time PCR. Treatment with AP-1 or NF-κB decoy ODN significantly decreased IL-1β, TNF-α, and MPO activities in the tissue contents, which coincided well with the results of our histological examinations (Figure 6a–c).

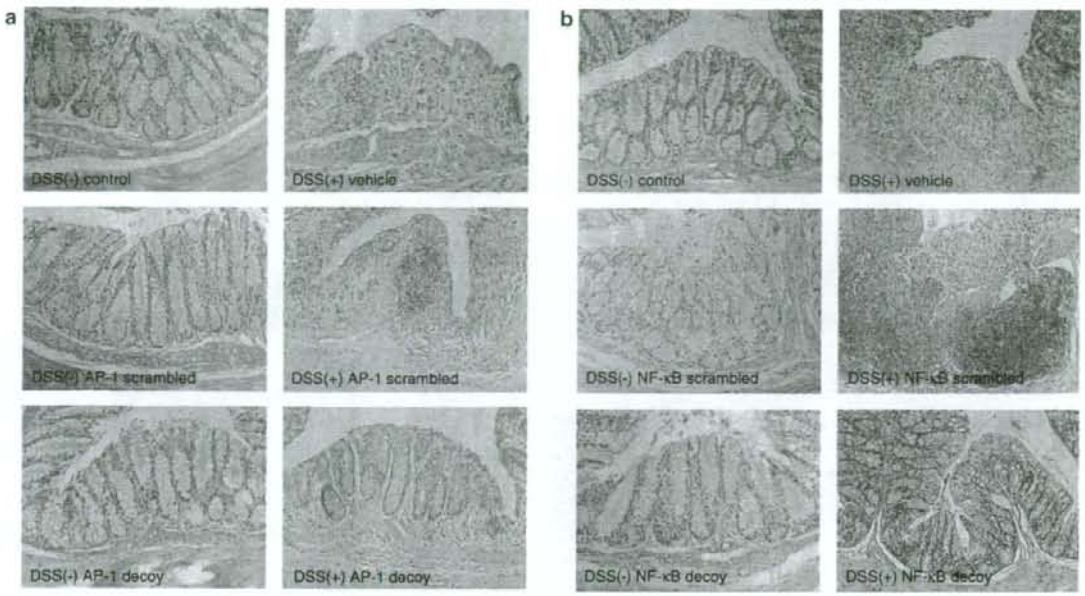

Figure 5 Effects of decoy ODNs on histological scores in mice with DSS-induced colitis. Distal colonic specimens were formalin-fixed and embedded in paraffin blocks, then 3-μm sections were stained with hematoxylin and eosin. (**a** and **b**) Representative histological images of samples from DSS-non-treated and -treated mice following treatment with or without decoy ODN or scrambled ODN (AP-1: 20 μg/mouse, NF-κB: 40 μg/mouse). (Original magnification × 100).

DISCUSSION

Studies of treatments with decoy ODNs targeting several transcriptional factors have demonstrated regulation of a variety of biological responses including inflammation and tumorigenesis in various organs.[33–40] Although AP-1 is a major immunoregulatory as well as proinflammatory transcription factor,[21,27–30,45–47] nothing is known to have been reported regarding the effect of AP-1 inhibition by a decoy ODN on intestinal inflammation. In the present study, we designed a ds decoy ODN binding to AP-1-specific nucleotide sequences and investigated its efficacy to prevent murine experimental DSS-induced colitis. Our findings demonstrated that AP-1 decoy ODN markedly inhibited DSS-induced colonic inflammation, indicating that AP-1 might be one of the potent targets for IBD therapy.

Recent advances in the elucidation of the pathogenesis of IBD have led to development of novel biological therapies that specifically inhibit molecules involved in the inflammatory cascade, including proinflammatory cytokines and their receptors, and adhesion molecules. Infliximab, a chimeric monoclonal antibody that binds with high affinity and specificity to TNF-α, has been demonstrated to be effective in both induction and maintenance therapy for patients with moderately to severely active CD, and is presently the only biological compound approved for CD therapy.[15,16,48,49] Newer therapeutic monoclonal antibodies targeting interferon (IFN)-γ,[50,51] IL-6 receptor,[18] IL-12 p40,[52] and α4-integrin[53] have also been developed, and clinical trials to evaluate the safety and efficiency of those agents for the treatment of IBD are being conducted. Although the development of therapeutic monoclonal antibodies is one of the most important advances in the care of IBD patients during the past decade, current therapies based on such biological agents are not entirely as effective as expected, as several untoward effects including immunogenicity, infusion reactions, and other serious adverse events have been reported.[13,16,17] Therefore, experimental approaches to develop new therapeutic options for IBD are encouraged.

In recent years, decoy ODNs bearing the consensus sequence of a specific transcription factor have been explored as new tools for manipulating gene expression in living cells. As a large number of transcription factors have already been identified and sequence-specific decoy ODNs are relatively easy to synthesize, the decoy approach represents a potential avenue for a wide range of clinical applications.[33,34] The multiplicity of target genes that are under the control of a single transcription factor also contributes to utility of decoy ODN strategies. Recent studies have demonstrated therapeutic applications of several decoy ODNs targeting transcription factors including NF-κB,[35–37] AP-1,[38–40] E2F,[54] Sp1,[55,56] and the signal transducer and activator of transcription (STAT) family.[57,58] There have also been a few reports suggesting an active role of AP-1 during the pathogenesis of IBD. Ishiguro *et al*[31] revealed that

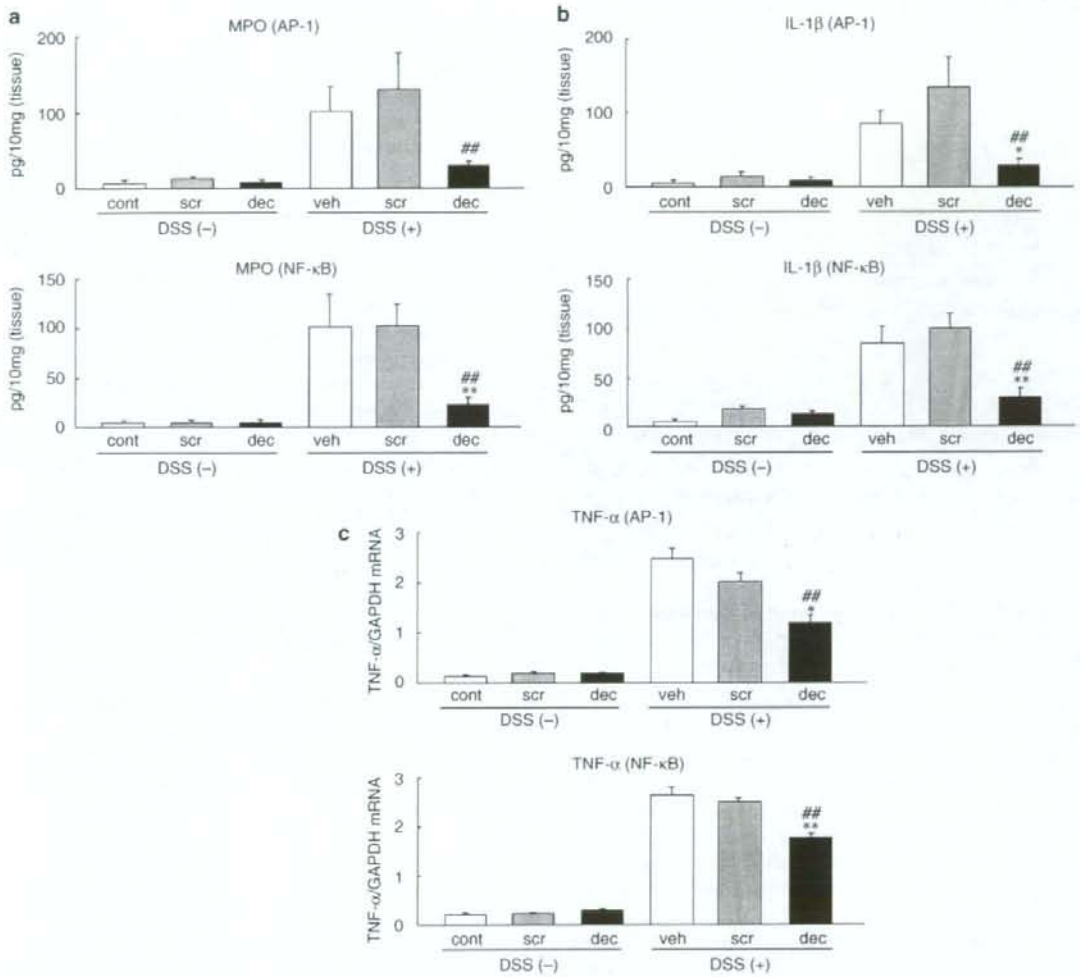

Figure 6 Effects of decoy ODNs on MPO activity (**a**), IL-1β contents (**b**), and TNF-α (**c**) in distal colonic samples collected from DSS-non-treated and -treated mice following treatment with or without decoy ODN or scrambled ODN (AP-1: 20 μg/mouse, NF-κB: 40 μg/mouse). Total protein and mRNA were extracted from each distal colonic tissue sample. MPO activity and IL-1β contents were evaluated using an EIA. Expression of TNF-α was examined by real-time PCR. Error bars indicate the s.e.m. values obtained independently from five mice. $^{*}P<0.05$, $^{**}P<0.01$, *vs* DSS(+) scrambled. $^{\#}P<0.05$, $^{\#\#}P<0.01$ *vs* DSS(+) vehicle.

AP-1-mediated expression of macrophage migration inhibitory factor (MIF) is involved in the glucocorticoid-resistant inflammatory process of UC. In addition, Andoh *et al*[32] recently reported that IL-22 is abundantly expressed in the colonic mucosa of IBD patients and activates the production of inflammatory cytokines, chemokines, and matrix metalloproteinases in colonic subepithelial myofibroblasts (SMEFs). They also demonstrated that IL-22-induced expression of inflammatory genes in SMEFs is mainly regulated by AP-1 signaling.

These observations suggest that control of AP-1 signaling may be a potent therapeutic target for treating IBD. In the present study, we constructed AP-1 decoy ODN and evaluated its anti-inflammatory effect on DSS-induced colitis in mice. As the therapeutic efficacy of NF-κB decoy ODN has been widely shown in a variety of studies,[33–37] the anti-inflammatory effect of NF-κB decoy ODN to prevent experimental colitis was also evaluated. Intraperitoneal treatment with AP-1 decoy ODN, but not scrambled ODN, significantly inhibited weight loss and shortening of the colon induced by DSS administration. Histological examinations clearly showed that crypt epithelial damage, as well as infiltration of lamina propria by polymorphonuclear and mononuclear cells were both markedly decreased in the AP-1 decoy

Table 1 Effect of decoy ODNs on histological inflammation

	Inflammation	Depth of injury	Crypt damage	Total
AP-1				
DSS(−) control	0.17 ± 0.17	0.17 ± 0.17	0.00 ± 0.00	0.33 ± 0.21
DSS(−) scrambled	0.33 ± 0.21	0.00 ± 0.00	0.00 ± 0.00	0.33 ± 0.21
DSS(−) decoy	0.17 ± 0.17	0.33 ± 0.21	0.00 ± 0.00	0.50 ± 0.22
DSS(+) vehicle	5.30 ± 0.90	4.20 ± 1.18	4.60 ± 1.18	14.10 ± 2.33
DSS(+) scrambled	4.60 ± 0.67	2.60 ± 0.27	4.90 ± 0.77	11.90 ± 1.17
DSS(+) decoy	2.20 ± 0.59*,#	2.10 ± 0.57	2.00 ± 0.64	6.30 ± 1.35*,#
NF-κB				
DSS(−) control	0.17 ± 0.17	0.17 ± 0.17	0.00 ± 0.00	0.33 ± 0.21
DSS(−) scrambled	0.33 ± 0.21	0.17 ± 0.17	0.00 ± 0.00	0.50 ± 0.22
DSS(−) decoy	0.17 ± 0.17	0.33 ± 0.21	0.00 ± 0.00	0.50 ± 0.22
DSS(+) vehicle	5.00 ± 1.14	3.50 ± 0.89	4.40 ± 1.07	13.40 ± 2.76
DSS(+) scrambled	4.30 ± 1.15	3.20 ± 0.84	4.60 ± 1.56	13.10 ± 3.59
DSS(+) decoy	1.40 ± 0.31*,#	1.60 ± 0.40	2.00 ± 0.45	5.10 ± 0.85*,#

AP-1 ODNs (scrambled; 20 μg per mouse, Decoy; 20 μg per mouse).
NF-κB ODNs (scrambled; 40 μg per mouse, Decoy; 40 μg per mouse).
*$P<0.05$ *vs* DSS(+) scrambled, #$P<0.05$ *vs* DSS(+) vehicle AP-1.

ODN-treated mice, which also coincided well with our findings regarding the colonic tissue contents of IL-1β, TNF-α, and MPO. Similar therapeutic effects were also observed in NF-κB decoy ODN-treated mice. Fichtner-Feigel *et al*[59] demonstrated the efficacy of NF-κB decoy ODN against murine experimental colitis induced by trinitrobenzene sulfonic acid (TNBS) and oxazolone, with prophylactic and therapeutic effects caused by apoptosis of $CD4^+$ cells, and suppressed production of inflammatory cytokines from colonic lamina propria cells was shown. Their findings support our view that decoy ODNs targeting transcription factors may become effective tools for preventing intestinal inflammation.

In the present study, we injected AP-1 decoy ODN into mice once a day from days 2 to 5 during the DSS administration period. The main purpose of our study was to evaluate whether AP-1 decoy ODN is applicable for induction IBD therapy, thus the decoy ODN was injected during the effector phase of DSS induction of colonic inflammation. We considered that this experimental protocol was useful to show the therapeutic potential of AP-1 decoy ODN to attenuate intestinal inflammation. On the other hand, AP-1 has also been recognized to play important roles in cell proliferation, migration, and differentiation in various organs.[21,27–30] Particularly, epithelial proliferation and migration are essential steps in the healing process of intestinal inflammation, which is regulated by a variety of AP-1-mediated genes. Therefore, blockade of AP-1-mediated signaling may influence mucosal regeneration during the healing of chronic intestinal inflammation including IBD, whereas the appropriate dosage period of AP-1 decoy ODN should be carefully evaluated for future clinical applications.

Host pattern recognition receptors can be activated by ds RNA or ds CpG-ODNs, and their signalling occurs in a type I IFN-dependent fashion. Anti-inflammatory response induced by such an ODN may be due to its immunostimulatory role. In the present study, we used decoy ODNs to inhibit the expression of pro-inflammatory genes whose promoters have binding sites for transcription factor AP-1. To avoid a possible immunostimulatory role of decoy ds ODNs, including corresponding scrambled ODNs, we selected sequences that were devoid of CPG motifs so that the ODNs would be less likely to produce a type-I IFN response. Moreover, we performed an *in vitro* control experiment to examine whether the anti-inflammatory responses induced by the AP-1 or NF-κB decoy ODNs were mediated through induction of type I IFN response. RT-PCR as well as an EIA were utilized for detection of IFN-β production in cells transfected with decoy ODNs, which showed that IFN-β production by cells transfected with AP-1 or NF-κB decoy ODNs was similar to that of those with scrambled ODNs. Moreover, the difference in IFN-β production remained insignificant even after stimulation of the ODN transfected cells with flagellin. The RT-PCR data were in line with the EIA results (data not shown). Therefore, it is not likely that the decoy ODNs inhibited intestinal inflammation through production of type-I IFN in the present experiments.

Recently, Suzuki *et al*[60] reported two clinical cases that utilized NF-κB decoy ODN, which showed its efficacy and safety for the prevention of restenosis after percutaneous coronary intervention. Indeed, decoy ODN strategies may have an effective therapeutic potential for a variety of diseases. However, there are several issues to be addressed before such clinical use is employed. One problem is related to how to efficiently deliver decoy ODNs in an organ- or cell-specific manner, because AP-1 and NF-κB are involved in a number of important physiological functions, whereas upregulation in certain organs or cells may be linked to pathological conditions like IBD that affect intestine and intestinal epithelia. Another is how to increase the stability of administrated decoy ODNs *in vivo*. ODN-based therapy requires high doses and frequent administrations, because ODNs are rapidly degraded *in vivo*. To resolve this issue, researchers have used end-modifications or conjugation of ODNs to increase their biological half life.[61–64] Further, viral envelopes including HVJ have been used to deliver ODNs *in vivo*, however, their safety remains unknown.[33,34,38] In the present study, injection of scrambled or decoy ODNs at 5, 20, or 40 μg per mouse did not show any influence on BW changes in mice without DSS treatment, thus those doses were considered to be safe for use in treatment of experimental colitis. Nevertheless, additional investigations addressing *in vivo* efficacy and safety should be carefully performed before ODNs can be considered for use in a clinical therapeutic strategy.